Reactions of Borane Anions with Polarized Acetylenes. Synthesis and Structural Characterization of New Polyhedral Di-, Tri-, and Tetracarbon Carboranes

Kai Su, Patrick J. Carroll, and Larry G. Sneddon*

Contribution from the Department of Chemistry, University of Pennsylvania, Philadelphia, Pennsylvania 19104-6323

Received June 16, 1993®

Abstract: A new synthetic strategy for achieving monocarbon or dicarbon insertions into polyhedral boron cage compounds, involving the reactions of polarized terminal alkynes with polyhedral borane and carborane anions, is reported. Monocarbon insertion is observed in the reactions of the *arachno*-6,8-$C_2B_7H_{12}^-$ anion with cyanoacetylene, methyl propiolate, and 3-butyn-2-one to give new polyhedral *arachno*-tricarbaboranes of the general formula *arachno*-6-(RCH_2)-5,6,7-$C_3B_7H_{12}$, where R = CN (**1**), C(O)OMe (**2**), or C(O)Me (**3**). Single-crystal X-ray studies of **1** and **2** have shown that these compounds, consistent with their 26 skeletal-electron counts, adopt 10-vertex *arachno* cage geometries based on an icosahedron missing two vertices, with the carbon atoms occupying adjacent positions on the open 6-membered face. **1** was found to undergo cage degradation with aqueous ammonium hydroxide to give the new hypho tricarbaborane, *hypho*-1-($NCCH_2$)-1,2,5-$C_3B_6H_{12}^-$ (**5**), the structure of which was established by a single-crystal X-ray study. Dicarbon insertion is observed in the reactions of *nido*-5,6-$C_2B_8H_{11}^-$ with methyl propiolate and *nido*-$B_{10}H_{13}^-$ with cyanoacetylene which result in the production of the isoelectronic *arachno*-tetracarbaborane, *arachno*-8-($CH_3OC(O)$)-7,8,9,10-$C_4B_8H_{13}$ (**6**), and *arachno*-dicarbaborane, *arachno*-8-(NC)-7,8-$C_2B_{10}H_{14}^-$ (**7**), clusters, respectively. Single-crystal X-ray studies show that, consistent with their arachno 30 skeletal-electron counts, both compounds adopt structures based on a bicapped hexagonal antiprism missing two vertices. The carbon atoms in both compounds occupy adjacent positions on the puckered six-membered open faces. Two-carbon insertion, accompanied by the loss of one boron, is observed in the reactions of *nido*-$B_{10}H_{13}^-$ with 3-butyn-2-one or methyl propiolate, which produced *nido*-7-(RC(O))-7,8-$C_2B_9H_{11}^-$ (R = Me (**8**) or MeO (**9**)) in high yields. In both monocarbon and dicarbon insertions, the reactions are proposed to involve an initial nucleophilic attack of the anion at the terminal alkyne carbon. The isolation of *arachno*-[*endo*-4-(NCCH=CH)]-6,8-$S_2B_7H_8^-$ (**10**) from the reaction of *arachno*-6,8-$S_2B_7H_8^-$ with cyanoacetylene provides additional support for this mechanism.

Introduction

In this paper we report both a new synthetic strategy by which carbon insertions into polyhedral boron anions may be achieved and the use of this method to synthesize important new classes of carboranes that have been inaccessible with conventional synthetic procedures. We have previously shown that either monocarbon or CN cage-insertion products may result from the reactions of nitriles with polyhedral borane anions.[1]

$$\textit{arachno}\text{-}6,8\text{-}S_2B_7H_8^- + MeC{\equiv}N \xrightarrow[(2)\ H^+]{(1)\ \text{reflux}} \textit{hypho}\text{-}5\text{-}CH_3\text{-}5,11,7,14\text{-}CNS_2B_7H_9 \quad (1)$$

$$\textit{arachno}\text{-}6,8\text{-}C_2B_7H_{12}^- + MeC{\equiv}N \xrightarrow[(2)\ H^+]{(1)\ \text{reflux},\ -NH_3} \textit{nido}\text{-}6\text{-}CH_3\text{-}5,6,9\text{-}C_3B_7H_{10} \quad (2)$$

In these reactions, we proposed that the key step was the initial nucleophilic attack of the borane anion at the positively charged nitrile carbon. Subsequent hydroboration of the nitrile and intramolecular condensation could then occur to produce (eq 1) the imine insertion products. Alternatively, complete reduction of the nitrile and deammination can take place resulting (eq 2) in monocarbon insertion. These results suggested that borane or carborane anions might be sufficiently nucleophilic to attack positive sites in other polarized triple bonds, such as those found in alkynes containing strongly electron withdrawing substituents, to form either mono- or dicarbon-insertion products. In a previous communication,[2] we reported the use of this strategy for the high-yield synthesis of the first example of a polyhedral *arachno*-tricarbaborane, *arachno*-6-($NCCH_2$)-5,6,7-$C_3B_7H_{12}$. We report here full details of this and related reactions of other polyhedral boron anions with polarized terminal alkynes that have resulted in new routes to di-, tri-, and tetracarbon carboranes.

Experimental Section

All manipulations were carried out with use of standard high vacuum or inert-atmosphere techniques as described by Shriver.[3]

Materials. Decaborane, *nido*-$B_{10}H_{14}$, was obtained from Callery Chemical Co. and sublimed before use. The compounds, *arachno*-6,8-$S_2B_7H_9$,[4] *arachno*-6,8-$C_2B_7H_{13}$,[5] and *nido*-5,6-$C_2B_8H_{12}$,[6] and their monoanions were prepared as reported previously. The anion, *nido*-$B_{10}H_{13}^-$, was generated from the reaction of *nido*-$B_{10}H_{14}$ with either KH or NaH as described below. Cyanoacetylene was prepared according to the literature method[7] from propiolamide, and its THF solution was stored at 0 °C as a stock solution. Methyl propiolate (97%), 3-butyn-2-one (99%), HCl-diethyl ether solution, PCl_3, D_2O, and bis(triphenylphosphoranylidene)ammonium chloride (PPN^+Cl^-) were purchased from Aldrich and used as received. Tetramethylammonium chloride (TMA^+Cl^-) was purchased from Aldrich and dried under vacuum at 110 °C for 2 h before use. THF, diethyl ether, hexane, and pentane were dried over Na/benzophenone and freshly distilled before use. Methylene chloride was dried over CaH_2 and distilled before use. Oil-dispersed sodium hydride was obtained from Aldrich, washed with dry hexane

* Abstract published in *Advance ACS Abstracts*, October 1, 1993.

(1) Kang, S. O.; Furst, G. T.; Sneddon, L. G. *Inorg. Chem.* **1989**, *28*, 2339–2347.

(2) Su, K.; Barnum, B.; Carroll, P. J.; Sneddon, L. G. *J. Am. Chem. Soc.* **1992**, *114*, 2730–2731.

(3) Shriver, D. F.; Drezdzon, M. A. *Manipulation of Air Sensitive Compounds*, 2nd ed.; Wiley: New York, 1986.

(4) Plešek, J.; Heřmánek, S.; Janoušek, Z. *Collect. Czech. Chem. Commun.* **1977**, *42*, 785–792.

(5) Garrett, P. M.; George, T. A.; Hawthorne, M. F. *Inorg. Chem.* **1969**, *8*, 2008–2009.

(6) Plešek, J.; Heřmánek, S. *Collect. Czech. Chem. Commun.* **1974**, *39*, 821–826.

(7) Moureu, C.; Bongrand, J. C. *Ann. Chim. (Paris)* **1920**, *9*, 14.

0002-7863/93/1515-10004$04.00/0

under a nitrogen atmosphere, and then vacuum dried. DCl was prepared by the reaction of PCl_3 with D_2O and purified by fractionation through a −78 °C trap into a −196 °C trap.

Physical Measurements. ^1H NMR spectra at 200.1 MHz, ^{11}B NMR spectra at 64.2 MHz, and ^{13}C NMR spectra at 50.3 MHz were obtained on a Bruker AF-200 spectrometer. ^{11}B NMR spectra at 160.5 MHz and ^{13}C NMR spectra at 125.7 MHz were obtained on a Bruker AM-500 spectrometer. All ^{11}B chemical shifts are referenced to external $BF_3{\cdot}O(C_2H_5)_2$ (0.0 ppm) with a negative sign indicating an upfield shift. All proton and carbon chemical shifts were measured relative to internal residual protons or carbons from the lock solvents and then referenced to Me_4Si (0.0 ppm). High- and low-resolution mass spectra were obtained on a VG-ZAB-E high-resolution mass spectrometer. Diffuse reflectance infrared spectra were obtained on a Perkin-Elmer 7770 Fourier transform spectrometer. Elemental analyses were performed at Robertson Microlit Laboratories Inc., Madison, NJ.

***arachno*-6-($NCCH_2$)-5,6,7-$C_3B_7H_{12}$ (1).** A 100-mL round-bottomed flask fitted with a vacuum stopcock was charged with 1.02 g (9.00 mmol) of *arachno*-6,8-$C_2B_7H_{13}$ and 0.20 g (8.33 mmol) of NaH. The flask was connected to the vacuum line and 50 mL of THF was vacuum distilled into the flask at −196 °C. The mixture was then allowed to warm to room temperature. After the gas evolution ceased (~20 min), the solution was filtered into another 100-mL flask under a N_2 atmosphere. A 0.50-g (9.80 mmol) sample of cyanoacetylene dissolved in 15 mL of THF was slowly dropped into the stirred solution. After 1 h at room temperature, the solution was acidified with 10 mL of HCl·diethyl ether solution (1 M) at −40 °C and then warmed to room temperature. The THF was vacuum evaporated and 20 mL of CH_2Cl_2 was added. The solution was filtered through a layer of silica gel to remove any insoluble materials. Vacuum evaporation of the solvent afforded 1.21 g (7.38 mmol, 82%) of crude product. Sublimation at 50 °C yielded 0.81 g (4.9 mmol, 54.4%) of a white, sweet-smelling solid. For **1**: mp, 71–72 °C; R_f = 0.60 in CH_2Cl_2/pentane (1:1 v/v); IR (KBr) 3028 (w), 2971 (w), 2943 (m), 2858 (m), 2645 (s), 2560 (vs), 2248 (m), 2006 (w), 1421 (m), 1386 (m), 1301 (m), 1250 (m), 1237 (w), 1209 (s), 1159 (s), 1067 (m), 1024 (s), 939 (s), 889 (m), 861 (w), 818 (m), 762 (m), 733 (w), 698 (w), 684 (m), 648 (w), 606 (w), 591 (w), 513 (w), 478 (w), 460 cm^{-1} (w). Anal. Calcd: C, 36.66; H, 8.55; N, 8.55. Found: C, 37.09; H, 9.00; N, 7.66. Exact mass calcd for $^{12}C_5{}^{11}B_7{}^{14}N^1H_{14}$ 165.1778, found 165.1780.

***arachno*-6-($NCCH_2$)-5,6,7-$C_3B_7H_{11}^-$ (1^-).** A 0.12-g (0.73 mmol) sample of *arachno*-6-($NCCH_2$)-5,6,7-$C_3B_7H_{12}$ and 0.05 g (1.25 mmol) of KH were placed in a 100 mL round-bottomed flask containing a magnetic stirbar. THF (20 mL) was vacuum distilled into the flask at −196 °C. The mixture was slowly warmed to room temperature. After gas evolution ceased, the solution was filtered under N_2 into another 100-mL flask. The ^{11}B NMR spectrum showed *arachno*-6-($NCCH_2$)-5,6,7-$C_3B_7H_{11}^-$ as the only product. In order to obtain a ^1H NMR spectrum of the anion, ~0.002 g of *arachno*-6-($NCCH_2$)-5,6,7-$C_3B_7H_{12}$ was dissolved in THF-d_8 and cooled to −40 °C. A ~0.001-g sample of KH was added and the mixture was allowed to warm to room temperature. As soon as the gas evolution ceased (~2 min at room temperature), the solution was filtered into a NMR tube under argon and its ^1H (and ^{11}B) NMR spectra taken.

***arachno*-6-($MeOC(O)CH_2$)-5,6,7-$C_3B_7H_{12}$ (2).** A 0.57-g (5.00 mmol) sample of *arachno*-6,8-$C_2B_7H_{13}$, 0.12 g (5.00 mmol) of NaH, and 35 mL of THF were used to generate *arachno*-6,8-$C_2B_7H_{12}^-$ as described above. The solution was filtered into another flask, and 0.46 g (5.51 mmol) of methyl propiolate was added via syringe. As evidenced by the disappearance of the starting material in the ^{11}B NMR spectrum of the reaction mixture, the reaction was complete in about 3 h at room temperature. The solution was then acidified with 5.2 mL of 1 M HCl·diethyl ether solution at −30 °C. After the mixture was warmed to room temperature, the solvent was vacuum evaporated and the remaining yellow oil was extracted with 40 mL of pentane. The pentane solution was then filtered through a layer of silica gel. Vacuum evaporation of the solvent resulted in the isolation of 0.56 g (2.85 mmol, 57%) of a light-yellow crude product. Recrystallization from pentane at −30 °C afforded 0.49 g of pure product. For **2**: mp, 43–44 °C; R_f = 0.84 in CH_2Cl_2/pentane (v/v 1:1); IR (KBr) 3446 (w), 3063 (m), 3007 (m), 2964 (m), 2921 (w), 2836 (m), 2751 (w), 2709 (w), 2638 (s), 2595 (vs), 2553 (vs), 2014 (w), 1730 (s), 1460 (s), 1441 (s), 1432 (s), 1389 (s), 1340 (s), 1241 (s), 1198 (s), 1177 (s), 1156 (m), 1091 (m), 1049 (m), 1021 (s), 993 (s), 950 (m), 886 (m), 815 (m), 765 (w), 730 (m), 694 (m), 638 (m), 602 (w), 574 (w), 517 (w), 464 (w). Anal. Calcd: C, 36.61; H, 8.36. Found: C, 35.73; H, 8.29. Exact mass calcd for $^{12}C_6{}^{11}B_7{}^{16}O_2{}^1H_{17}$ 198.8000, found 198.7971.

***arachno*-6-($MeC(O)CH_2$)-5,6,7-$C_3B_7H_{12}$ (3).** A 0.25-g (2.19 mmol) sample of *arachno*-6,8-$C_2B_7H_{13}$, 0.07 g (2.91 mmol) of NaH, and 20 mL of THF were used to generate *arachno*-6,8-$C_2B_7H_{12}^-$ as described above. The solution was filtered into another flask and 0.17 g (2.50 mmol) of 3-butyn-2-one was added via syringe. After the reaction mixture was stirred at room temperature for ~1 h, it was acidified with 2.5 mL of 1 M HCl·diethyl ether solution at 0 °C and then slowly warmed to room temperature. The solvent was vacuum evaporated and the remaining yellow oil was extracted with 30 mL of pentane. Filtration of the pentane solution through a layer of silica gel, followed by vacuum evaporation of the solvent, resulted in the isolation of 0.20 g (1.11 mmol, 50.7%) of a light-yellow crude product. Recrystallization from pentane at −30 °C afforded 0.15 g of a pure product. For **3**: mp, 51–52 °C; R_f = 0.62 in CH_2Cl_2/pentane (1:1 v/v); IR (KBr) 3056 (m), 3000 (w), 2957 (s), 2915 (s), 2855 (s), 2645 (s), 2574 (vs), 2021 (m), 1705 (vs), 1407 (s), 1379 (s), 1358 (s), 1322 (m), 1258 (w), 1237 (w), 1166 (s), 1081 (s), 1038 (s), 953 (s), 890 (s), 861 (w), 812 (s), 762 (m), 734 (m), 698 (m), 648 (m), 606 (m), 514 (w), 475 cm^{-1} (m). Anal. Calcd: C, 39.00; H, 9.41. Found: C, 39.72; H, 9.22. Exact mass calcd for $^{12}C_6{}^{11}B_7{}^{16}O^1H_{17}$ 182.1931, found 182.1927.

***arachno*-6-($NCCH{=}CH$)-6,8-$C_2B_7H_{11}^-$ (4).** A 0.33-g (2.93 mmol) sample of *arachno*-6,8-$C_2B_7H_{13}$, 0.07 g (2.92 mmol) of NaH, and 20 mL of THF were used to generate *arachno*-6,8-$C_2B_7H_{12}^-$ as described above. A cyanoacetylene/THF solution (5.7 mL, 0.52 mmol/mL) was then added dropwise at room temperature. The colorless solution immediately turned light yellow. Analysis of the reaction mixture by ^{11}B NMR after 40 min showed that the starting carborane anion was completely consumed. At this time, a 0.32-g (2.92 mmol) sample of $Me_4N^+Cl^-$ was added to the flask and the mixture was stirred for 1 h. The solvent was then vacuum evaporated and the residue was dissolved in 20 mL of methylene chloride. After filtration, the methylene chloride solution was added dropwise to 50 mL of diethyl ether, which resulted in the precipitation of a pale yellow solid. The product was filtered, washed with two 8-mL portions of diethyl ether, and dried under vacuum to give 0.39 g (2.40 mmol, 81.9%) of air-sensitive product. For **4**: IR (KBr) 3057 (m), 3028 (m), 3007 (m), 2510 (vs), 2326 (w), 2198 (s), 1925 (w), 1854 (w), 1578 (s), 1479 (vs), 1415 (m), 1294 (m), 1223 (m), 1188 (s), 1138 (s), 1053 (s), 989 (s), 947 (m), 897 (w), 798 (m), 712 (w), 506 (w), 482 cm^{-1} (w). Anal. Calcd: C, 46.22; H, 9.41; N, 11.99. Found: C, 44.97; H, 11.06; N, 11.43.

Acidification of *arachno*-6-($NCCH{=}CH$)-6,8-$C_2B_7H_{11}^-$ with DCl. A 0.31-g (2.91 mmol) sample of *arachno*-6,8-$C_2B_7H_{13}$, 0.07 g (2.92 mmol) of NaH, and 30 mL of THF were used to generate *arachno*-6,8-$C_2B_7H_{12}^-$ as described above. After the solution was filtered into another flask under N_2, a cyanoacetylene/THF solution (5.3 mL, 0.56 M, 2.97 mmol) was added dropwise at room temperature. The solution was allowed to stir for 1 h. The flask was then attached to the vacuum line and 3.14 mmol of gaseous DCl, which had been measured in a calibrated volume, was condensed into the reaction flask at −196 °C. The mixture was slowly warmed to room temperature and stirred for 1 h. The THF solvent was then vacuum evaporated and replaced with 20 mL of diethyl ether. After filtration through a layer of silica gel, vacuum evaporation of the solvent gave 0.30 g (1.82 mmol, 62.5%) of light-yellow crude product. Sublimation at 50 °C give 0.21 g of white solid.

PPN^+*hypho*-1-($NCCH_2$)-1,2,5-$C_3B_6H_{12}^-$ (5). A 0.30-g (1.83 mmol) sample of *arachno*-6-($NCCH_2$)-5,6,7-$C_3B_7H_{12}$ was dissolved in 20 mL of methylene chloride in a 100-mL flask. An aqueous 37% NH_4OH (3 mL) solution was then added. After the mixture was stirred at room temperature for 23 min, its ^{11}B NMR spectrum showed complete conversion to the product. At this point, 1.05 g (1.83 mmol) of PPN^+Cl^- was added and the solution stirred for 15 min. The CH_2Cl_2 solution was then separated from the water and washed with an additional 15 mL of H_2O. After 10 mL of diethyl ether was added to the CH_2Cl_2 solution, heptane was added dropwise until the solution became slightly cloudy. Evaporation of the solvents under argon resulted in the crystallization of 0.80 g (1.16 mmol, 63.4%) of **5**. For **5**: IR (KBr) 3057 (m), 2957 (s), 2929 (s), 2820 (m), 2545 (s), 2496 (vs), 2234 (m), 1975 (m), 1904 (w), 1826 (m), 1590 (m), 1580 (s), 1436 (vs), 1287 (vs), 1188 (m), 1167 (vs), 1025 (m), 998 (m), 970 (m), 918 (m), 890 (m), 797 (m), 748 (s), 726 (vs), 691 (vs), 549 (vs), 528 (vs), 499 cm^{-1} (vs). Anal. Calcd: C, 71.22; H, 6.37; N, 4.06. Found: C, 70.70; H, 6.41; N, 3.85. The Me_4N^+ salt was made by exchanging the NH_4^+ cation with $Me_4N^+Cl^-$.

***arachno*-8-($CH_3OC(O)$)-7,8,9,10-$C_4B_8H_{13}$ (6).** A 100-mL round-bottomed flask fitted with a vacuum stopcock was charged with 0.95 g (7.76 mmol) of *nido*-5,6-$C_2B_8H_{12}$ and 0.33 g (13.75 mmol) of NaH. THF (40 mL) was then vacuum distilled into the flask at −196 °C and

the mixture was allowed to warm to room temperature. After gas evolution ceased (~20 min), the solution containing *nido*-5,6-$C_2B_8H_{11}^-$ was filtered into another 100-mL two-neck flask under a N_2 atmosphere. A 0.66-g (7.85 mmol) sample of methyl propiolate was dropped into the stirred solution at 0 °C. The mixture was then stirred at room temperature for ~1.5 h. The solution was next acidified with HCl·diethyl ether solution (8.2 mL, 1 M) at −78 °C and slowly warmed to room temperature. The THF was then vacuum evaporated and the residue extracted with 40 mL of pentane. The solution was filtered through a layer of silica gel and the filtrate concentrated. Crystallization by slow cooling to −20 °C afforded 0.92 g (4.45 mmol, 57.3%) of a crude product. Recrystallization from cold pentane produced 0.70 g of a white, crystalline solid. For **6**: mp 67–68 °C; R_f = 0.40 in CH_2Cl_2/pentane (v/v 1:2); IR (KBr) 3070 (s), 2975 (m), 2900 (m), 2858 (m), 2602 (vs), 2560 (vs), 2518 (s), 1719 (s), 1436 (s), 1329 (m), 1258 (s), 1230 (s), 1099 (m), 1042 (m), 992 (m), 914 (m), 779 (m), 751 (w), 716 (w), 673 (w), 588 cm^{-1} (w). Anal. Calcd: C, 34.87; H, 7.74. Found: C, 35.70; H, 7.74. Exact mass calcd for $^{12}C_6{}^{11}B_8{}^{16}O^1H_{16}$ 208.1895, found 208.1907.

PPN$^+$*arachno*-8-(NC)-7,8-$C_2B_{10}H_{14}^-$ (7). A 100-mL round-bottomed flask fitted with a vacuum stopcock was charged with 1.00 g (8.19 mmol) of *nido*-$B_{10}H_{14}$ and 0.43 g (10.75 mmol) of KH. THF (30 mL) was vacuum distilled into the flask at −196 °C and the mixture was warmed to room temperature. After gas evolution ceased (~30 min), the yellow solution containing *nido*-$B_{10}H_{13}^-$ was immediately filtered into another 100-mL two-neck flask under a N_2 atmosphere. A cyanoacetylene/THF solution (19.5 mL, 0.44 mmol/mL) was then added to the mixture at 0 °C. After the reaction mixture was stirred for 14 h at 0 °C, 4.86 g (8.47 mmol) of PPN$^+$Cl$^-$ was added and the solution was stirred at room temperature for an additional hour. The THF was then vacuum evaporated and 20 mL of CH_2Cl_2 was added. After filtration of the solution, ~20 mL of diethyl ether was added and the solution was filtered again. At this point, heptane was slowly added to the filtrate with stirring until small needles appeared. Slow evaporation of the remaining solvent afforded 5.07 g (7.13 mmol, 87.1%) of crystalline PPN$^+$*arachno*-8-(NC)-7,8-$C_2B_{10}H_{14}^-$. For **7**: IR (KBr) 3085 (m), 3056 (m), 2929 (m), 2886 (w), 2830 (m), 2532 (vs), 2205 (s), 1968 (w), 1904 (w), 1819 (w), 1776 (w), 1670 (w), 1585 (s), 1486 (s), 1436 (s), 1379 (vs), 1308 (s), 1189 (s), 1117 (s), 996 (s), 748 (s), 719 (vs), 691 (vs), 535 (vs), 499 cm^{-1} (s). Anal. Calcd: C, 65.84; H, 6.19; N, 3.94. Found: C, 66.11; H, 5.92; N, 3.63.

PPN$^+$*nido*-7-($CH_3C(O)$)-7,8-$C_2B_9H_{11}^-$ (8). A 100-mL round-bottomed flask fitted with a vacuum stopcock was charged with 0.44 g (11.00 mmol) of KH and 30 mL of THF. A 1.04-g (8.52 mmol) sample of *nido*-$B_{10}H_{14}$ dissolved in 8 mL of THF was added dropwise. After gas evolution ceased (~20 min), the yellow solution containing *nido*-$B_{10}H_{13}^-$ was filtered into another 100-mL flask under a N_2 atmosphere. A 1.16-g (17.00 mmol) sample of 3-butyn-2-one was added via syringe at room temperature. The reaction was very exothermic, causing the THF to reflux. After the mixture was stirred for 40 min, 4.89 g (8.52 mmol) of PPN$^+$Cl$^-$ was added and the solution was stirred for an additional hour. The solvent was then vacuum evaporated and 20 mL of CH_2Cl_2 was added. After filtration, ~20 mL of diethyl ether was added to the solution and the solution was filtered again. Heptane was then added dropwise to the stirred filtrate until the onset of crystallization was observed. Slow evaporation of the solvent afforded 4.57 g (6.41 mmol, 75.2%) of crystalline PPN$^+$*nido*-7-($CH_3C(O)$)-7,8-$C_2B_9H_{11}^-$. For **8**: IR (KBr) 3049 (m), 3021 (m), 2525 (vs), 2042 (w), 1979 (w), 1908 (w), 1882 (w), 1780 (w), 1666 (s), 1589 (m), 1482 (s), 1439 (s), 1354 (s), 1255 (vs), 1191 (s), 1113 (s), 1028 (m), 1000 (s), 801 (m), 744 (s), 723 (s), 695 (s), 553 (s), 532 (s), 496 cm^{-1} (s). Anal. Calcd: C, 67.22; H, 6.16; N, 1.96. Found: C, 66.93; H, 6.16; N, 1.91.

Me_4N^+*nido*-7-($CH_3OC(O)$)-7,8-$C_2B_9H_{11}^-$ (9). A 100-mL round-bottomed flask fitted with a vacuum stopcock was charged with 0.44 g (10.00 mmol) of KH and 30 mL of THF. A 1.04-g (8.52 mmol) sample of *nido*-$B_{10}H_{14}$ dissolved in 15 mL of THF was added dropwise. After gas evolution ceased (~20 min), the yellow solution containing *nido*-$B_{10}H_{13}^-$ was filtered into another 100-mL flask under a N_2 atmosphere. A 1.43-g (17.0 mmol) sample of methyl propiolate was added via syringe. After the solution was heated at reflux for 2 h, the solvent was vacuum evaporated and the residue was dissolved in 20 mL of H_2O. Addition of 1.10 g (10.05 mmol) of $Me_4N^+Cl^-$ in 5 mL of H_2O resulted in a light-yellow precipitate. The precipitate was washed with two 5-mL portions of H_2O and dried in vacuo, which afforded 1.60 g (6.42 mmol, 75.4%) of product. For **9**: IR (KBr) 3042 (m), 2950 (m), 2532 (vs), 1708 (vs), 1481 (vs), 1436 (s), 1290 (vs), 1213 (s), 1078 (s), 1021 (s), 946 (s), 812 (m), 776 (m), 723 cm^{-1} (m). Anal. Calcd: C, 36.19; H, 9.80; N, 5.28. Found: C, 33.98; H, 9.49; N, 4.71.

***arachno*-[*endo*-4-(NCCH=CH)]-6,8-$S_2B_7H_8^-$ (10).** A solution of Na^+6,8-$S_2B_7H_9^-$ was prepared by the reaction of 0.23 g (1.55 mmol) of *arachno*-6,8-$S_2B_7H_9$ and 0.15 g (6.25 mmol) of NaH in 20 mL of THF, as previously described.[4] After initial gas evolution ceased (about 1 h), the anion solution was filtered into another 100-mL two-neck flask under a N_2 atmosphere. To this stirred solution was added 0.20 g (3.92 mmol) of cyanoacetylene dissolved in 9 mL of THF over ~15 min, and the combined solution was then allowed to stir for 1 h at room temperature. At this point, the ^{11}B NMR spectrum showed quantitative conversion to the product. A 0.18-g (1.64 mmol) sample of $Me_4N^+Cl^-$ was then added to the reaction solution. After being stirred for 1 h, the reaction mixture was filtered. The addition of 20 mL of hexane to the filtrate resulted in the precipitation of a yellow solid. The product was filtered and washed with two 5-mL portions of hexane. Further vacuum drying overnight gave 0.29 g (1.06 mmol, 68.4%) of product. For **10**: IR (KBr) 3075 (w), 2964 (w), 2567 (vs), 2510 (vs), 2411 (s), 2198 (vs), 1528 (m), 1486 (vs), 1450 (w), 1358 (w), 1262 (w), 1046 (m), 1018 (m), 705 (m), 684 (m), 634 (w), 584 (w), 482 cm^{-1} (w). Anal. Calcd: C, 30.38; H, 8.03; N, 10.23. Found: C, 30.45; H, 7.39; N, 9.95.

Acidification of *arachno*-[*endo*-4-(NCCH=CH)]-6,8-$S_2B_7H_8^-$. A 0.20-g (0.27 mmol) sample of the PPN$^+$ salt of *arachno*-[*endo*-4-(NCCH=CH)]-6,8-$S_2B_7H_8^-$ was charged into a 100-mL round-bottomed flask equipped with a vacuum stopcock. The flask was connected to the vacuum line and 15 mL of CH_2Cl_2 was vacuum distilled into the flask. A slight excess of gaseous HCl (0.30 mmol) was then condensed into the flask at −196 °C, and the mixture was slowly warmed to −78 °C. Vigorous gas evolution was observed, and the ^{11}B NMR spectrum taken after 1 h showed only decomposition products.

Crystallographic Data for Compounds 2 and 5–8. Single crystals of **2** and **6** were grown by slowly cooling saturated pentane solutions to 0 °C. Single crystals of **5**, **7**,and **8** were grown by slow evaporation of CH_2Cl_2/diethyl ether/heptane solutions under Ar. Suitably sized crystals were placed inside capillary tubes which were then sealed with glue.

Collection and Reduction of the Data. X-ray intensity data were collected at 295 K on an Enraf-Nonius CAD-4 diffractometer employing graphite-monochromated Cu Kα radiation (λ = 1.54184 Å) with use of the ω–2θ scan technique. For each compound three standard reflections measured every 3500 s of X-ray exposure showed less than 10% intensity decay over the course of data collection. A linear decay correction was applied. The intensity data were corrected for Lorentz and polarization effects, but not for absorption.

Solution and Refinement of the Structure. All calculations were performed on a DEC MicroVAX 3100 computer using the Enraf-Nonius Molen structure package. The full-matrix least-squares refinement was phased on F, and the function minimized was $\sum w(|F_o| - |F_c|)^2$. The weights (w) were taken as $4F_o^2/(\sigma(F_o^2))^2$ where $|F_o|$ and $|F_c|$ are the observed and calculated structure factor amplitudes. The neutral-atom scattering factors and complex anomalous dispersion corrections are those stored in the SDP package. Agreement factors are defined as $R = \sum||F_o| - |F_c||/\sum|F_o|$ and $Rw = (\sum w(|F_o| - |F_c|)^2/\sum w|F_o|^2)^{1/2}$. The structures were solved by direct methods (MULTAN 11/82). Subsequent Fourier maps led to the locations of all non-hydrogen atoms. Anisotropic refinements followed by difference Fourier syntheses resulted in the location of all cage hydrogens, except the bridge hydrogens in **7**. The positions of the remaining hydrogens and the bridge-hydrogens in **7** were then calculated. Hydrogen atoms were not refined, but were included as constant contributions to the structure factors. The final refinements included anisotropic thermal parameters for non-hydrogen atoms and fixed isotropic thermal parameters for the hydrogen atoms (6 Å^2). Final difference Fouriers were featureless.

The cage atoms in **8** were disordered by rotation about the C7–C12 bond. This resulted in a boron atom occupancy of 20% in the 12-position (B12) and 80% in the 3-position (B3). Similarly, the atom in the 8-position (CB8) was 80% C and 20% B, and the atom in the 11-position (BC11) was 20% C and 80% B.

Crystal and refinement data are given in Table II. Final positional parameters are given in Tables III–VII. Selected intramolecular bond distances are presented in Tables VIII–XII.

Results

Monocarbon Insertions: New Tricarbaboranes. *arachno*-6-(RCH_2)-5,6,7-$C_3B_7H_{12}$, where R = CN (1), C(O)Me (2), or C(O)OMe (3). The *arachno*-6,8-$C_2B_7H_{12}^-$ anion reacted with cyanoacetylene, methyl propiolate or 3-butyn-2-one in THF solution

Table I. NMR Data

compounds	nucleus	δ (multiplicity, assignment, *J* (Hz))
arachno-6-($NCCH_2$)-5,6,7-$C_3B_7H_{12}$, **1**	$^{11}B^{d,f}$	10.7 (d, B2, J_{BH} 184), −3.8 (d of d, B8,10, J_{BH} 149, $J_{BH(br)}$ 26), −25.4 (d, B1,3, J_{BH} 167), −26.8 (d, B9, J_{BH} ~200), −41.0 (d, B4, J_{BH} 151)
	^{11}B–$^{11}B^{a,f}$	crosspeaks: B2–B1,3; B8,10–B1,3; B8,10–B9; B8,10–B4; B1,3–B4; B9–B4
	$^{13}C^{b,f}$	116.7 (s, C12), 39.2 (d, C6, J_{CH} 170), 27.1 (t, CH_2, J_{CH} 137), 11.5 (d, C5,7, J_{CH} 170)
	$^{1}H(^{11}B)^{c,f}$	4.05 (B2H or B4H), 2.90 (B1,3H or B8,10H), 2.82 (d, CH_2, J_{HH} 7.0), 2.12 (t, B9H, $J_{HH(br)}$ 8.6), 1.98 (B1,3H or B8,10H), 1.34 (C5,7H), 0.19 (B2H or B4H), −0.11 (t, C6H, J_{HH} 7.0), −3.04 (BHB)
K^+*arachno*-6-($NCCH_2$)-5,6,7-$C_3B_7H_{11}^-$, **1**$^-$	$^{11}B^{d,g}$	8.4 (d, 1, J_{BH} 182), −3.5 (d, 2, J_{BH} 131), −25.7 (t, B, J_{BH} 88), −29.8 (d, 3, J_{BH} 144)
	$^{1}H^{c,g}$	2.87 (d, CH_2, J_{HH} 7.7), 0.67 (C5,7H, br), 0.31 (C6H, br), −3.06 (q, *endo*-B9H, J_{HB} 70, br)
	$^{1}H(^{11}B)^{c,g,h}$	3.88 (BH), 2.87 (d, CH_2, J_{BH} 7.1), 2.39 (BH), 1.51 (BH), 0.68 (C5,7H), 0.32 (m, C6H, br), −3.06 (s, *endo*-B9H)
arachno-6-(NCCDH)-5,6,7-$C_3B_7H_{12}$, **1-d**$_1$	$^{11}B^{a,f}$	10.7 (d, B2, J_{BH} 188), −3.7 (d, B8,10, J_{BH} 147), −25.1 (d, B1,3, J_{BH} 163), −26.1 (d, B9, J_{BH} obscured), −41.1 (d, B4, J_{BH} 148)
	$^{13}C(^{1}H)^{b,f}$	116.7 (s, C12), 38.8 (s, C6), 26.6 (t, CDH, J_{CD} 21), 11.3 (m, C5,7, J_{CB} 29)
	$^{1}H(^{11}B)^{c,f}$	4.05 (B2H or B4H), 2.82 (d, CH_2, J_{HH} 7.0), 2.78 (B1,3H or B8,10H), 2.12 (t, B9H, $J_{HH(br)}$ 8.6), 1.97 (B1,3H or B8,10H), 1.34 (C5,7H), 0.18 (B2H or B4H), −0.12 (d, C6H, J_{HH} 7.0), −3.05 (BHB)
arachno-6-($MeOC(O)CH_2$)-5,6,7-$C_3B_7H_{12}$, **2**	$^{11}B^{a,f}$	10.0 (d, B2, J_{BH} 187), −4.0 (d of d, B8,10, J_{BH} 149, $J_{BH(br)}$ 34), −26.3 (d, B1,3, J_{BH} 162), −27.2 (d, B9, J_{BH} obscured), −41.0 (d, B4, J_{BH} 146)
	$^{13}C^{b,f}$	170.6 (s, C12), 51.8 (q, CH_3, J_{CH} 149), 42.7 (t, CH_2, J_{CH} 131), 39.0 (d, C6, J_{CH} 164), 11.8 (d, C5,7, J_{CH} 165)
	$^{1}H(^{11}B)^{c,f}$	4.00 (B2H or B4H), 3.66 (s, CH_3), 2.77 (d, CH_2, J_{HH} 6.6), 2.72 (B1,3H or B8, 10H), 1.94 (t, B9H, $J_{HH(br)}$ 8.6), 1.83 (B1,3H or B8,10H), 1.23 (C5,7H), 0.16 (B2H or B4H), 0.00 (t, C6H, J_{HH} 7.2), −3.05 (BHB)
arachno-6-($MeC(O)CH_2$)-5,6,7-$C_3B_7H_{12}$, **3**	$^{11}B^{a,f}$	9.5 (d, B2, J_{BH} 186), −4.0 (d of d, B8,10, J_{BH} 148, $J_{BH(br)}$ 31), −26.8 (d, B1,3, J_{BH} 162), −27.5 (d, B9, J_{BH} obscured), −41.1 (d, B4, J_{BH} 147)
	$^{13}C(^{1}H)^{b,f}$	178.2 (C12), 51.9 (CH_3), 37.7 (C6), 29.5 (CH_2), 11.8 (C5,7)
	$^{1}H(^{11}B)^{c,f}$	3.93 (B2H or B4H), 2.92 (d, CH_2, J_{HH} 6.6), 2.73 (B1,3H or B8,10H), 2.10 (s, CH_3), 1.94 (m, B9H, $J_{HH(br)}$ 7.0), 1.80 (B1,3H or B8,10H), 1.14 (C5,7H), 0.14 (B2H or B4H), 0.05 (t, C6H, J_{HH} 6.6), −3.05 (BHB)
Me_4N^+*arachno*-6-(NCCH=CH)-6,8-$C_2B_7H_{11}^-$, **4**	$^{11}B^{a,f}$	8.6 (d, J_{BH} 110), 1.2 (d, J_{BH} 140), −8.4 (d, J_{BH} 134), −16.9 (d of d, J_{BH} 140, $J_{BH(br)}$ 30), −36.4 (d, J_{BH} 135), −42.4 (d, J_{BH} 125), −44.4 (d, J_{BH} 150)
	$^{1}H(^{11}B)^{c,f,h}$	4.71 (m, vinyl CH's), 3.64 (BH), 3.29 (Me_4N^+), 2.90 (BH), 2.74 (m, br, cage-CH), 2.48 (BH), 2.08 (BH), 1.42 (m, br, cage CH), 0.56 (BH), −0.06 (BH), −4.23 (BHB)
PPN^+*hypho*-1-($NCCH_2$)-1,2,5-$C_3B_6H_{12}^-$, **5**	$^{11}B^{d,f}$	−6.6 (d, B7,9, J_{BH} 112), −30.4 (d, B8, J_{BH} 151), −32.1 (d, B10,11, J_{BH} 122), −51.2 (d, B12, J_{BH} 133)
	^{11}B–$^{11}B^{a,f}$	crosspeaks: B12–B10,11; B12–B8; B12–B7,9; B8–B7,9; B7,9–B12
	$^{13}C^{e,f}$	121.0 (m, C14), 42.6 (d, C1, J_{CH} 133), 25.9 (t, C13, J_{CH} 133), 17.4 (d, C2,5, J_{CH} 145)
	$^{1}H(^{11}B)^{c,f}$	2.08 (B7,9H), 1.75 (d, C13H, J_{HH} 6.6), 1.55 (m, B8H, $J_{HH(br)}$ 7.1), 0.82 (d, B10,11H, $J_{HH(br)}$ 8.80), 0.66 (t, C1H, J_{HH} 7.0), 0.48 (s, C2,5H), −1.06 (B12H), −2.53 (2, BHB (B7,9–B8)), −3.01 (t, 1, BHB (B10–B11), J_{HH} 11.8)
arachno-8-($CH_3OC(O)$)-7,8,9,10-$C_4B_8H_{13}$, **6**	$^{11}B^{d,f}$	46.8 (d, J_{BH} 175), 13.6 (d, J_{BH} 162), −10.2 (d, J_{BH} 175), −20.5 (d, J_{BH} 146), −21.9 (d, J_{BH} 169), −26.0 (d of d, J_{BH} 140, $J_{BH(br)}$ 64), −27.4 (d, J_{BH} 150), −40.1 (d, J_{BH} 153)
	$^{13}C^{e,f}$	171.4 (CA), 53.5 (q, CH_3, J_{CH} 148), 38.8 (d, C9 or C10, J_{CH} 176), 30.5 (s, C8), 18.8 (d, C9 or C10, J_{CH} 159), −20.4 (t, C7, J_{CH} 155)
	$^{1}H(^{11}B)^{c,f}$	5.70 (BH), 4.05 (BH), 3.76 (CH_3), 3.40 (m, cage-CH), 2.88 (BH), 2.22 (BH), 2.07 (m, cage-CH), 1.58 (BH), 1.47 (d, *exo*-C7H, J_{HH} 15.4), 1.06 (t, *endo*-C7H, J_{HH} 12), 0.95 (BH), 0.69 (BH), −0.93 (m, BHB)
PPN^+*arachno*-8-(NC)-7,8-$C_2B_{10}H_{14}^-$, **7**	$^{11}B^{d,f}$	28.0 (d, 1, J_{BH} 156), 16.5 (d, 1, J_{BH} 143), −6.2 (d, 2, J_{BH} 144), −8.8 (d, 1, J_{BH} 135), −21.3 (d, 1, J_{BH} 130), −23.4 (d, 1, J_{BH} 140), −25.0 (d, 1, J_{BH} 147), −31.3 (d, 1, J_{BH} 157), −32.3 (d, 1, J_{BH} 144)
	$^{13}C^{e,f}$	128.3 (CA), 3.37 (s, C8), −4.59 (t, C7, J_{CH} 137)
	$^{1}H(^{11}B)$	4.66 (BH), 3.68 (BH), 2.51 (B12H), 2.31 (BH), 2.13 (BH), 1.29 (2, BH), 1.14 (d of d, *exo*-C7H), 0.93 (BH), 0.68 (d of d, *endo*-C7H), 0.52 (BH), 0.26 (BH), −1.93 (BHB, B11–B12), −3.95 (BHB, B9–B10)
PPN^+*nido*-7-($MeC(O)$)-7,8-$C_2B_9H_{11}^-$, **8**	$^{11}B^{d,f}$	−7.3 (d, J_{BH} 138), −7.5 (d, J_{BH} 138), −11.7 (d, J_{BH} ~167), −12.7 (d, J_{BH} 142), −17.1 (d, J_{BH} 143), −18.5 (d, J_{BH} 156), −22.3 (d, J_{BH} 148), −31.2 (d of d, J_{BH} 124, $J_{BH(br)}$ 36), −33.7 (d, J_{BH} 139)
	$^{13}C^{e,f}$	210.5 (s, C12), 66.7 (m, C7, J_{CB} 48), 40.8 (d of m, C8, J_{CH} 162, J_{CB} 48), 26.7 (q, CH_3, J_{CH} 128, J_{CB} 50)
	$^{1}H(^{11}B)^{c,f}$	2.57 (C8H), 2.34 (BH), 2.09 (BH), 2.07 (CH_3), 1.81 (BH), 1.63 (BH), 1.41 (BH), 1.30 (BH), 1.17 (BH), 0.72 (BH), 0.17 (BH), −2.66 (BHB, (B9–10))
TMA^+*nido*-7-($MeOC(O)$)-7,8-$C_2B_9H_{11}^-$, **9**	$^{11}B^{d,f}$	−7.8 (d, 2, J_{BH} 135), −12.8 (d, 2, J_{BH} 119), −17.9 (d, 2, J_{BH} 140), −22.6 (d, 1, J_{BH} 148), −31.0 (d of d, 1, J_{BH} 131, J_{BHbr} 41), −34.4 (d, 1, J_{BH} 140)
	$^{13}C^{e,f}$	172.2 (s, C12), 56.0 (q, Me_4N^+, J_{CH} 148), 55.7 (s, C7), 51.7 (q, CH_3, J_{CH} 147), 42.7 (d, C8, J_{CH} 170)
	$^{1}H(^{11}B)^{c,f}$	3.57 (CH_3), 3.27 (Me_4N^+), 2.47 (C8H), 2.22 (BH), 2.09 (BH), 1.91 (BH), 1.57 (BH), 1.37 (BH), 1.16 (2, BH), 0.64 (BH), 0.15 (BH), −2.66 (BHB, (B9–10))
arachno-[*endo*-4-(NCCH=CH)]-6,8-$S_2B_7H_8^-$, **10**	$^{11}B^{a,f}$	11.5 (d, B5,9, J_{BH} 148), 0.2 (d, B7, J_{BH} 156), −7.1 (d, B1, J_{BH} 133), −28.6 (d, B2,3, J_{BH} 168), −38.0 (d, B4, J_{BH} 108)
	^{11}B–$^{11}B^{a,f}$	crosspeaks: B5,9–B1; B5,9–B2,3; B5,9–B4; B1–B2,3; B1–B4
	$^{13}C^{e,f}$	189.5 (d of q, C1, J_{CB} 62, J_{CH} ~115), 122.8 (s, C3), 92.0 (d, C2, J_{CH} 167) 56.2 (q, NMe_4^+, J_{CH} 154)
	$^{13}C(^{1}H, -85°)^{b,f}$	190.0 (s, C1), 123.3 (s, C3), 92.9 (s, C2), 56.3 (Me_4N^+)
	$^{1}H(^{11}B)^{c,f}$	5.70 (m, CH), 4.87 (m, CH), 3.48 (B5,9H and B7H), 3.29 (Me_4N^+), 2.50 (B1H), 1.65 (B2,3H), 0.77 (B4H)

[a] 64.2 MHz. [b] 50.3 MHz. [c] 200.1 MHz. [d] 160.5 MHz. [e] 125.7 MHz. [f] CD_2Cl_2. [g] THF-d_8. [h] Not all terminal BH's were observed.

Table II. Crystallographic Data Collection and Structure Refinement Information

	2	5	6	7	8
space group	*Pbca*	$P2_1/c$	$P\bar{1}$	$P\bar{1}$	$P2_1/n$
Z	8	4	2	2	4
cell constants					
a, Å	11.059(1)	10.614(1)	7.263(2)	12.260(2)	10.142(1)
b, Å	10.820(1)	10.938(1)	7.632(1)	12.266(2)	21.953(3)
c, Å	19.348(3)	13.974(2)	10.823(4)	14.824(2)	18.527(3)
α, deg			98.98(2)	110.59(1)	
β, deg		108.88(1)	98.37(3)	105.35(1)	103.30(1)
γ, deg			92.88(2)	93.41(2)	
V, Å^3	2315.1(8)	1535.1(6)	584.7(6)	1983(1)	4014(2)
μ, cm^{-1}	4.74	3.48	4.82	12.08	12.11
D_{calc}, g/cm^3	1.130	0.983	1.174	1.190	1.181
$F(000)$	832	496	216	744	1496
radiation, λ, Å	Cu Kα (1.54184)	Cu Kα (1.54184)	Cu Kα (1.54184)	Cu Kα (1.54184)	Cu Kα (1.54184)
θ range, deg	2.0–65.0	2.0–65.0	2.0–65.0	2.0–65.0	2.0–65.0
scan mode	ω–2θ	ω–2θ	ω–2θ	ω–2θ	ω–2θ
h, k, l collected	+12, +12, +22	±12, −12, +16	±8, ±8, −12	+14, ±14, ±17	+11, +25, ±21
no. of reflecns measured	2267	2885	2107	7107	7446
no. of unique reflecns	1767	2607	1990	6756	6807
no. with $F_o^2 > 3.0\sigma(F_o)$	1217	1867	1206	4322	5498
no. of parameters	204	238	210	478	531
R_1	0.054	0.069	0.064	0.053	0.046
R_2	0.061	0.098	0.074	0.067	0.067

Table III. Refined Positional Parameters for *arachno*-6-(MeOC(O)CH$_2$)-5,6,7-C$_3$B$_7$H$_{12}$, **2**

atom	x	y	z	B_{eq},[a] Å^2
B1	1.0188(3)	0.1163(4)	0.7226(2)	5.16(8)
B2	0.9278(3)	0.2369(3)	0.7072(2)	5.07(8)
B3	1.0760(3)	0.2510(3)	0.6901(2)	5.00(7)
B4	1.1381(3)	0.1092(3)	0.6624(2)	4.67(7)
B8	1.1009(3)	0.2272(3)	0.5994(2)	4.78(8)
B9	1.0993(3)	0.0625(4)	0.5809(2)	5.03(8)
B10	1.0078(3)	0.0089(3)	0.6529(2)	4.76(7)
C5	0.8927(2)	0.0959(3)	0.6736(1)	4.21(6)
C6	0.8688(2)	0.1903(2)	0.6135(1)	3.62(5)
C7	0.9737(2)	0.2848(2)	0.6272(2)	4.47(6)
C11	0.7435(2)	0.2480(3)	0.6108(2)	4.64(6)
C12	0.6485(2)	0.1595(2)	0.5872(1)	3.79(5)
C15	0.4394(2)	0.1410(3)	0.5626(2)	6.04(8)
O13	0.6631(2)	0.0512(2)	0.5770(1)	5.24(5)
O14	0.5437(1)	0.2167(2)	0.5795(1)	4.96(4)
H1	1.020(2)	0.075(2)	0.773(1)	7.8(8)*
H2	0.865(2)	0.291(2)	0.741(1)	6.6(7)*
H3	1.127(2)	0.327(2)	0.713(1)	6.9(7)*
H4	1.231(2)	0.085(2)	0.677(1)	5.5(6)*
H5	0.823(2)	0.062(2)	0.693(1)	5.7(6)*
H6	0.884(2)	0.152(2)	0.569(1)	3.2(5)*
H7	0.956(2)	0.363(2)	0.615(1)	5.6(6)*
H8	1.175(2)	0.284(2)	0.576(1)	6.1(6)*
H9	1.163(2)	0.009(2)	0.553(1)	5.5(6)*
H10	1.010(2)	−0.086(2)	0.668(1)	6.5(6)*
H89	1.060(2)	0.147(2)	0.548(1)	7.0(7)*
H910	1.002(2)	0.009(2)	0.582(1)	5.2(6)*
H11a	0.746(2)	0.313(2)	0.578(1)	6.1(7)*
H11b	0.722(2)	0.284(2)	0.655(1)	6.8(7)*
H15a	0.454(3)	0.103(3)	0.517(2)	11.0(1)*
H15b	0.424(3)	0.078(3)	0.603(2)	10.0(1)*
H15c	0.380(3)	0.201(3)	0.562(2)	10.1(9)*

[a] Entries with an asterisk were refined isotropically. $B_{eq} = {}^4/_3[\beta_{11}a^2 + \beta_{22}b^2 + \beta_{33}c^2 + \beta_{12}ab\cos\gamma + \beta_{13}ac\cos\beta + \beta_{23}bc\cos\alpha]$.

Table IV. Refined Positional Parameters for Me$_4$N$^+$*hypho*-1-(NCCH$_2$)-1,2,5-C$_3$B$_6$H$_{12}^-$, **5**

atom	x	y	z	B_{eq},[a] Å^2
B7	−0.1163(3)	0.3097(3)	0.0329(2)	5.27(7)
B8	−0.1752(4)	0.2252(4)	−0.0827(2)	6.62(9)
B9	−0.2280(3)	0.0848(3)	−0.0447(3)	6.37(8)
B10	−0.2832(3)	0.1119(3)	0.0733(3)	5.72(8)
B11	−0.2106(3)	0.2569(3)	0.1219(2)	4.95(7)
B12	−0.2834(3)	0.2354(3)	−0.0130(2)	5.23(7)
C1	−0.0311(2)	0.1023(2)	0.1273(2)	4.36(5)
C2	−0.0584(2)	0.2389(2)	0.1337(2)	4.20(5)
C5	−0.1596(3)	0.0362(2)	0.0653(2)	5.70(7)
C13	0.0220(3)	0.0464(3)	0.2338(2)	5.71(6)
C14	0.1491(3)	0.0982(3)	0.2920(2)	6.27(7)
N15	0.2499(3)	0.1391(3)	0.3340(2)	8.97(8)
N16	0.3783(2)	0.1428(2)	0.6509(1)	4.52(4)
C17	0.4423(4)	0.0642(4)	0.5959(3)	10.6(1)
C18	0.4580(5)	0.2476(5)	0.6970(5)	10.2(2)
C19	0.2478(5)	0.1828(7)	0.5887(5)	13.1(2)
C20	0.3562(7)	0.0752(7)	0.7354(5)	13.7(2)
C18′	0.259(1)	0.090(1)	0.661(1)	9.9(4)
C19′	0.369(2)	0.260(1)	0.596(1)	13.0(6)
C20′	0.463(2)	0.159(2)	0.747(1)	12.0(5)
H1	0.044(2)	0.089(2)	0.100(2)	5.1(5)
H2	0.005(2)	0.274(2)	0.179(1)	4.8(5)
H5	−0.151(3)	−0.041(3)	0.080(2)	9.1(8)
H7	−0.106(2)	0.407(3)	0.024(2)	7.7(7)
H8	−0.238(3)	0.267(3)	−0.168(2)	11.0(9)
H9	−0.299(4)	0.026(3)	−0.109(3)	14(1)
H10	−0.384(2)	0.081(2)	0.063(2)	6.7(6)
H11	−0.255(3)	0.333(3)	0.155(2)	9.0(8)
H12	−0.378(3)	0.279(3)	−0.051(2)	8.4(7)
H78	−0.074(2)	0.255(2)	−0.044(2)	6.3(6)
H89	−0.126(2)	0.124(2)	−0.084(2)	7.4(7)
H1011	−0.248(2)	0.161(2)	0.162(2)	5.6(6)
H13a	−0.041(2)	0.060(2)	0.270(2)	7.1(6)
H13b	0.031(3)	−0.042(3)	0.228(2)	8.7(8)

[a] $B_{eq} = {}^4/_3[\beta_{11}4a^2 + \beta_{22}b^2 + \beta_{33}c^2 + \beta_{12}ab\cos\gamma + \beta_{13}ac\cos\beta + \beta_{23}bc\cos\alpha]$.

to yield, following protonation, a series of new tricarbaboranes of general formula *arachno*-6-(RCH$_2$)-5,6,7-C$_3$B$_7$H$_{12}$.

$$\textit{arachno}\text{-}6,8\text{-}C_2B_7H_{12}^- + HC{\equiv}CR \xrightarrow[(2)\ H^+]{(1)\ RT} \textit{arachno}\text{-}6\text{-}(RCH_2)\text{-}5,6,7\text{-}C_3B_7H_{12} \quad (3)$$

R = CN (**1**), C(O)OMe (**2**), or C(O)Me (**3**)

According to the ^{11}B NMR spectra of the reaction mixtures, the tricarbaboranes were the sole products. The compounds were isolated as slightly air-sensitive white crystalline solids in yields ranging from 51 to 82%. The ester and ketone derivatives are readily soluble in hydrocarbons and can be purified by recrystallization from pentane. The cyano derivative has limited solubility in pentane, but it is volatile and can be purified by slow sublimation at elevated temperatures.

The compositions of the tricarbaboranes were initially established by both elemental analyses and exact mass measurements. All three compounds exhibited intense cutoff envelopes consistent with their formulations.

We reported the structural confirmation of **1** in an earlier

Table V. Refined Positional Parameters for *arachno*-8-($CH_3OC(O)$)-7,8,9,10-$C_4B_8H_{13}$, **6**

atom	*x*	*y*	*z*	B_{eq},[a] Å^2
B1	0.1344(7)	0.0664(5)	0.1969(5)	5.3(1)
B2	0.0850(6)	0.2524(6)	0.1288(4)	4.9(1)
B3	0.3038(6)	0.2448(6)	0.2259(4)	4.9(1)
B4	0.2525(7)	0.1325(6)	0.3495(5)	6.0(1)
B5	0.0171(7)	0.0717(6)	0.3247(5)	5.7(1)
B6	−0.0916(7)	0.1430(6)	0.1893(4)	5.5(1)
B11	−0.1107(7)	0.2595(6)	0.3451(5)	6.2(1)
B12	−0.1139(7)	0.3788(6)	0.2037(5)	6.1(1)
C7	0.0530(6)	0.5302(5)	0.2209(4)	5.6(1)
C8	0.2378(5)	0.4517(4)	0.2627(3)	4.27(8)
C9	0.2606(5)	0.3612(5)	0.3757(3)	5.09(9)
C10	0.1004(6)	0.2621(5)	0.4205(3)	5.7(1)
CA	0.4055(5)	0.5716(4)	0.2582(3)	4.82(9)
CB	0.5429(6)	0.7569(5)	0.1334(4)	7.3(1)
OA	0.3934(4)	0.6289(3)	0.1471(2)	6.08(6)
OB	0.5333(4)	0.6151(4)	0.3418(3)	7.05(7)
HB1	0.157(5)	−0.051(4)	0.130(3)	6.8(9)*
HB2	0.089(5)	0.281(4)	0.030(3)	8(1)*
HB3	0.443(4)	0.240(4)	0.200(3)	5.5(8)*
HB4	0.357(5)	0.076(5)	0.404(3)	9(1)*
HB5	−0.035(5)	−0.032(5)	0.365(3)	8(1)*
HB6	−0.215(5)	0.063(4)	0.123(3)	6.9(9)*
HB11	−0.232(5)	0.224(4)	0.385(3)	6.8(9)*
HB12	−0.244(5)	0.396(5)	0.156(3)	8(1)*
HB1112	−0.141(6)	0.412(5)	0.319(4)	10(1)*
H7a	0.043(4)	0.629(4)	0.293(3)	5.7(8)*
H7b	0.067(5)	0.559(5)	0.131(3)	10(1)*
H9	0.366(4)	0.414(4)	0.446(3)	5.5(8)*
H10	0.124(5)	0.281(4)	0.505(3)	7.1(9)*
HCBa	0.642(6)	0.713(5)	0.121(4)	11(1)*
HCBb	0.485(7)	0.797(7)	0.045(5)	16(2)*
HCBc	0.548(5)	0.852(4)	0.204(3)	8(1)

[a] Entries with an asterisk were refined isotropically. $B_{eq} = {}^4/_3[\beta_{11}a^2 + \beta_{22}b^2 + \beta_{33}c^2 + \beta_{12}ab\cos\gamma + \beta_{13}ac\cos\beta + \beta_{23}bc\cos\alpha]$.

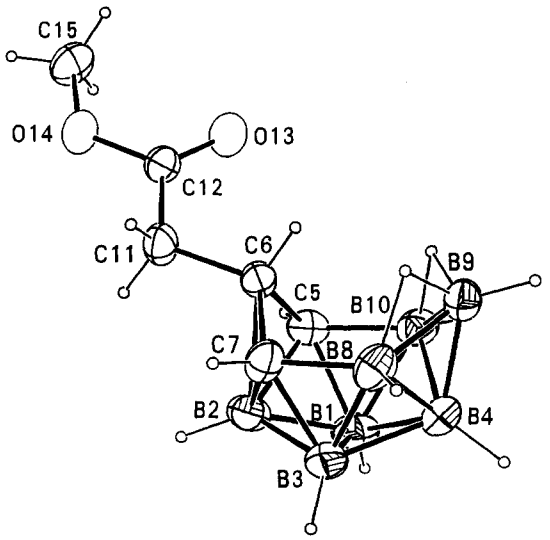

Figure 1. ORTEP drawing of the structure of *arachno*-6-(MeO(O)-CH_2)-5,6,7-$C_3B_7H_{12}$, **2**.

communication.[2] A single-crystal X-ray study of *arachno*-6-($MeOC(O)CH_2$)-5,6,7-$C_3B_7H_{12}$ (**2**), as shown in the ORTEP drawing in Figure 1, has confirmed that it adopts a similar cage structure. Consistent with their 26 skeletal-electron counts, **1** and **2** adopt cage geometries based on an icosahedron missing two vertices (Figure 2), similar to those which have been either confirmed or proposed for other 10-vertex *arachno* cage systems such as the borane, $B_{10}H_{14}^{2-}$,[8] monocarbaborane 6-$CB_9H_{14}^-$,[9] and

(8) Kendall, D. S.; Lipscomb, W. N. *Inorg. Chem.* **1973**, *12*, 546–551.
(9) Štíbr, B.; Jelinek, T.; Plešek, J.; Heřmánek, S. *J. Chem. Soc., Chem. Commun.* **1987**, 963–964.

Table VI. Refined Positional Parameters for PPN^+*arachno*-8-(NC)-7,8-$C_2B_{10}H_{14}^-$, **7**

atom	*x*	*y*	*z*	B_{eq},[a] Å^2
B1	1.0485(5)	0.3348(5)	0.6620(4)	7.4(2)
B2	0.9338(6)	0.3853(6)	0.6946(6)	9.0(2)
B3	1.0219(6)	0.4749(5)	0.6700(4)	7.4(2)
B4	1.1624(4)	0.4563(5)	0.7202(4)	7.8(1)
B5	1.1558(4)	0.3464(4)	0.7677(4)	6.6(1)
B6	1.0141(5)	0.2968(4)	0.7561(4)	6.6(1)
B9	1.1138(5)	0.5808(4)	0.7909(4)	6.7(1)
B10	1.2001(5)	0.4903(5)	0.8476(5)	7.8(2)
B11	1.1137(5)	0.3884(5)	0.8750(4)	7.6(2)
B12	0.9624(4)	0.4017(4)	0.8458(4)	6.7(1)
C7	0.9237(5)	0.5177(5)	0.8340(4)	11.0(2)
C8	0.9731(3)	0.5520(3)	0.7631(3)	5.6(1)
CA	0.9138(4)	0.6418(4)	0.7383(4)	7.1(1)
N1	0.8660(4)	0.7134(3)	0.7221(4)	9.5(1)
P1	0.45202(7)	0.83470(7)	0.71549(6)	3.39(2)
P2	0.63530(7)	1.03659(7)	0.74117(6)	3.26(2)
C13	0.3166(3)	0.8804(3)	0.7211(2)	3.56(7)
C14	0.2132(3)	0.8028(3)	0.6691(3)	4.8(1)
C15	0.1113(3)	0.8442(4)	0.6709(3)	6.3(1)
C16	0.1097(3)	0.9591(4)	0.7234(3)	6.2(1)
C17	0.2098(4)	1.0362(3)	0.7757(3)	6.1(1)
C18	0.3140(3)	0.9978(3)	0.7743(3)	4.84(9)
C19	0.4224(3)	0.7068(3)	0.6021(2)	3.61(8)
C20	0.3776(3)	0.5965(3)	0.5970(3)	5.0(1)
C21	0.3458(4)	0.5012(3)	0.5069(3)	6.1(1)
C22	0.3593(4)	0.5128(4)	0.4219(3)	6.4(1)
C23	0.4031(4)	0.6198(4)	0.4255(3)	6.1(1)
C24	0.4354(3)	0.7176(3)	0.5153(3)	4.49(9)
C25	0.5085(3)	0.7883(3)	0.8188(2)	3.58(8)
C26	0.6185(3)	0.7609(3)	0.8346(3)	4.8(1)
C27	0.6645(4)	0.7241(3)	0.9131(3)	5.8(1)
C28	0.6023(4)	0.7144(4)	0.9740(3)	6.1(1)
C29	0.4931(4)	0.7392(4)	0.9584(3)	6.1(1)
C30	0.4457(3)	0.7775(3)	0.8804(3)	4.8(1)
C31	0.7468(3)	1.0613(3)	0.8553(2)	3.54(8)
C32	0.7191(3)	1.0547(3)	0.9387(3)	4.70(9)
C33	0.8028(4)	1.0805(4)	1.0282(3)	6.1(1)
C34	0.9154(4)	1.1127(4)	1.0370(3)	6.5(1)
C35	0.9445(3)	1.1208(4)	0.9556(3)	6.0(1)
C36	0.8614(3)	1.0954(3)	0.8651(3)	4.66(9)
C37	0.7011(3)	1.0045(3)	0.6421(2)	3.35(7)
C38	0.7210(3)	1.0858(3)	0.6009(2)	4.42(9)
C39	0.7776(4)	1.0586(4)	0.5275(3)	5.6(1)
C40	0.8141(3)	0.9521(4)	0.4967(3)	5.6(1)
C41	0.7947(3)	0.8714(4)	0.5386(3)	5.4(1)
C42	0.7381(3)	0.8968(3)	0.6102(3)	4.50(9)
C43	0.5830(3)	1.1743(3)	0.7583(2)	3.38(7)
C44	0.4769(3)	1.1757(3)	0.6965(3)	4.60(9)
C45	0.4338(3)	1.2802(3)	0.7132(3)	5.6(1)
C46	0.4946(4)	1.3828(3)	0.7898(3)	5.6(1)
C47	0.6005(4)	1.3832(3)	0.8494(3)	5.4(1)
C48	0.6455(3)	1.2792(3)	0.8350(3)	4.48(9)
N2	0.5347(2)	0.9349(2)	0.7143(2)	4.64(7)

[a] $B_{eq} = {}^4/_3[\beta_{11}a^2 + \beta_{22}b^2 + \beta_{33}c^2 + \beta_{12}ab\cos\gamma + \beta_{13}ac\cos\beta + \beta_{23}bc\cos\alpha]$.

dicarbaborane 6,9-$C_2B_8H_{14}$[10] analogues. The three carbons are adjacent in the 5,6,7-vertex positions on the puckered six-membered open face, with the C6 carbons having both *endo*-hydrogens and *exo* substituents (*exo*-$MeOC(O)CH_2^-$, **2**; *exo*-$NCCH_2^-$, **1**). Bridging hydrogen atoms are also present at the B8–B9 and B9–B10 edges.

Although their gross cage structures are consistent with skeletal-electron counting predictions, examination of the interatomic cage distances for both **1** and **2** reveals similar features that may be attributed to the hybrid organic–inorganic nature of the clusters. The C6–C5 (1.552(6) Å for **1** and 1.570(4) Å for **2**) and C6–C7 (1.549(6) Å for **1** and 1.569(3) Å for **2**) distances are longer than those normally observed between adjacent cage carbons, and are

(10) (a) Štíbr, B.; Plešek, J.; Heřmánek, S. *Collect. Czech. Chem. Commun.* **1974**, *39*, 1805–1809. (b) Štíbr, B.; Plešek, J.; Heřmánek, S. *Chem. Ind. (London)* **1972**, 963–964. (c) Wermer, J. R.; Hosmane, N. S.; Alexander, J. J.; Siriwardane, U.; Shore, S. G. *Inorg. Chem.* **1986**, *25*, 4351–4354.

Table VII. Refined Positional Parameters for PPN^+*nido*-7-(MeC(O))-7,8-$C_2B_9H_{11}^-$, **8**

atom	x	y	z	B_{eq},[a] Å^2
C7	0.7254(3)	0.1335(1)	0.8784(1)	4.94(6)
CB8	0.7079(3)	0.1765(1)	0.8092(2)	5.85(7)
C12	0.6646(4)	0.0728(2)	0.8653(2)	7.19(8)
C13	0.6875(5)	0.0283(2)	0.9253(3)	10.9(1)
B1	0.9550(3)	0.2020(2)	0.8973(2)	5.07(7)
B2	0.8802(3)	0.1439(2)	0.9377(2)	4.66(6)
B4	0.8465(4)	0.2199(2)	0.8114(2)	5.97(8)
B5	0.8458(3)	0.2671(2)	0.8877(2)	5.53(8)
B6	0.8683(3)	0.2189(2)	0.9674(2)	5.10(7)
B9	0.6897(4)	0.2472(2)	0.8289(2)	5.96(8)
B10	0.7078(3)	0.2505(2)	0.9282(2)	6.14(8)
BC11	0.7264(3)	0.1712(2)	0.9545(2)	5.77(7)
B3	0.8632(4)	0.1461(2)	0.8414(2)	4.92(8)
B12	0.624(2)	0.1867(8)	0.874(1)	6.7(4)
O1	0.5979(3)	0.0578(1)	0.8047(2)	11.88(8)
P1	0.66117(5)	0.12925(2)	0.22696(3)	3.08(1)
P2	0.75910(5)	0.07640(3)	0.37531(3)	3.10(1)
N1	0.6591(2)	0.10977(8)	0.30897(9)	3.38(4)
C14	0.4892(2)	0.13320(9)	0.1736(1)	3.22(4)
C15	0.4626(2)	0.1365(1)	0.0966(1)	4.44(5)
C16	0.3314(3)	0.1420(1)	0.0558(1)	5.17(6)
C17	0.2262(3)	0.1437(1)	0.0906(2)	5.22(6)
C18	0.2509(3)	0.1411(2)	0.1660(2)	5.66(7)
C19	0.3827(2)	0.1355(1)	0.2084(1)	4.57(5)
C20	0.7433(2)	0.0751(1)	0.1790(1)	3.64(4)
C21	0.8674(2)	0.0845(1)	0.1616(1)	4.62(5)
C22	0.9249(3)	0.0381(2)	0.1287(2)	6.21(7)
C23	0.8616(3)	−0.0167(1)	0.1136(2)	6.50(7)
C24	0.7384(3)	−0.0266(1)	0.1312(2)	6.35(7)
C25	0.6791(3)	0.0194(1)	0.1637(1)	4.85(6)
C26	0.7323(2)	0.2038(1)	0.2246(1)	3.62(4)
C27	0.7513(3)	0.2391(1)	0.2877(2)	6.41(7)
C28	0.7985(4)	0.2983(1)	0.2863(2)	8.73(9)
C29	0.8270(3)	0.3219(1)	0.2240(2)	6.82(8)
C30	0.8089(3)	0.2874(1)	0.1617(2)	6.00(7)
C31	0.7613(3)	0.2289(1)	0.1611(1)	4.99(6)
C32	0.6749(2)	0.0114(1)	0.4029(1)	3.42(4)
C33	0.5603(2)	−0.0120(1)	0.3557(1)	4.49(5)
C34	0.4972(3)	−0.0627(1)	0.3770(2)	5.43(6)
C35	0.5486(3)	−0.0900(1)	0.4435(2)	5.72(6)
C36	0.6624(3)	−0.0681(1)	0.4898(2)	6.66(7)
C37	0.7254(3)	−0.0170(1)	0.4704(1)	5.42(6)
C38	0.9144(2)	0.0509(1)	0.3540(1)	3.55(4)
C39	0.9342(3)	−0.0092(1)	0.3371(1)	4.71(5)
C40	1.0515(3)	−0.0258(1)	0.3152(2)	6.26(7)
C41	1.1467(3)	0.0172(2)	0.3098(2)	6.33(7)
C42	1.1281(2)	0.0765(2)	0.3269(2)	5.66(7)
C43	1.0126(2)	0.0943(1)	0.3484(1)	4.55(5)
C44	0.8040(2)	0.1247(1)	0.4553(1)	3.49(4)
C45	0.7085(2)	0.1654(1)	0.4692(1)	4.35(5)
C46	0.7369(3)	0.2008(1)	0.5327(2)	5.62(6)
C47	0.8593(3)	0.1965(1)	0.5817(1)	5.73(7)
C48	0.9551(3)	0.1573(1)	0.5683(2)	5.84(7)
C49	0.9291(3)	0.1205(1)	0.5055(1)	4.90(6)
H1	1.060(2)	0.206(1)	0.901(1)	6.3(6)
H2	0.940(2)	0.102(1)	0.969(1)	6.3(7)
H3	0.899(3)	0.114(2)	0.815(2)	10(1)
H4	0.883(4)	0.232(2)	0.760(2)	12(1)
H5	0.899(2)	0.314(1)	0.893(1)	6.0(6)
H6	0.929(3)	0.235(1)	1.021(1)	7.2(7)
H8	0.648(3)	0.158(2)	0.761(2)	9.7(9)
H9	0.623(3)	0.277(1)	0.785(2)	8.2(8)
H10a	0.666(3)	0.287(1)	0.963(2)	8.7(8)
H10b	0.625(3)	0.218(1)	0.892(2)	6.1(8)
H11	0.676(3)	0.148(1)	1.008(2)	7.9(8)

[a] $B_{eq} = {}^4/_3[\beta_{11}a^2 + \beta_{22}b^2 + \beta_{33}c^2 + \beta_{12}ab\cos\gamma + \beta_{13}ac\cos\beta + \beta_{23}bc\cos\alpha]$.

in the range expected for carbon–carbon single bonds. The C6–B2 distances are quite long (2.015(8) Å for **1** and 1.991(4) Å for **2**), and the B2–B1, B2–B3, and B1–B3 distances are unusually short (~1.64–1.71 Å), when compared to similar distances in the isoelectronic analogues above or to those in *nido*-$B_{10}H_{14}$.[11]

(11) Tippe, A.; Hamilton, W. C. *Inorg. Chem.* **1969**, *8*, 464–470.

Table VIII. Bond Distances (Å) in *arachno*-6-($MeOC(O)CH_2$)-5,6,7-$C_3B_7H_{12}$, **2**

B1–B2	1.675(5)	B4–B8	1.814(5)	C5–C6	1.570(4)
B1–B3	1.709(5)	B4–B9	1.712(5)	C5–H5	0.931(23)
B1–B4	1.762(5)	B4–B10	1.814(5)	C6–C7	1.569(3)
B1–B10	1.786(5)	B4–H4	1.099(22)	C6–C11	1.520(3)
B1–C5	1.701(4)	B8–B9	1.817(5)	C6–H6	0.966(19)
B1–H1	1.065(25)	B8–C7	1.631(4)	C7–H7	0.904(24)
B2–B3	1.678(4)	B8–H8	1.125(25)	C11–C12	1.492(3)
B2–C5	1.703(4)	B8–H89	1.391(26)	C11–H11a	0.951(23)
B2–C6	1.991(4)	B9–B10	1.817(5)	C11–H11b	0.973(25)
B2–C7	1.708(4)	B9–H9	1.055(24)	C12–O13	1.200(3)
B2–H2	1.116(24)	B9–H89	1.195(26)	C12–O14	1.323(3)
B3–B4	1.765(5)	B9–H910	1.218(25)	C15–O14	1.452(3)
B3–B8	1.797(5)	B10–C5	1.633(4)	C15–H15a	0.984(33)
B3–C7	1.702(4)	B10–H10	1.069(27)	C15–H15b	1.055(34)
B3–H3	1.093(24)	B10–H910	1.363(24)	C15–H15c	0.921(30)

Table IX. Selected Bond Distances (Å) in Me_4N^+*hypho*-1-($NCCH_2$)-1,2,5-$C_3B_6H_{12}^-$, **5**

B7–B11	1.921(5)	B7–B12	1.865(4)	B7–C2	1.550(4)
B7–H7	1.086(28)	B7–H78	1.420(26)	B8–B9	1.774(5)
B8–B12	1.732(5)	B8–H8	1.250(28)	B8–H78	1.088(21)
B8–H89	1.223(27)	B9–B10	1.943(6)	B9–B12	1.849(5)
B9–C5	1.565(4)	B9–H9	1.166(34)	B9–H89	1.430(28)
B10–B11	1.798(4)	B10–B12	1.811(5)	B10–C5	1.586(4)
B10–H10	1.084(23)	H10–H1011	1.287(21)	B11–B12	1.807(4)
B11–C2	1.582(4)	B11–H11	1.131(30)	B11–H1011	1.306(23)
B12–H12	1.081(25)	C1–C2	1.531(3)	C1–C5	1.539(3)
B7–B8	1.790(5)	C1–C13	1.537(3)	C1–H1	0.998(24)
C2–H2	0.855(18)	C5–H5	0.865(29)	C13–C14	1.447(4)
C13–H13a	0.973(29)	C13–H13b	0.976(28)	C14–N15	1.132(4)

Table X. Bond Distances (Å) in *arachno*-8-($CH_3OC(O)$)-7,8,9,10-$C_4B_8H_{13}$, **6**

B1–B2	1.729(7)	B4–C9	1.721(6)	B12–HB12	1.281(40)
B1–B3	1.747(6)	B4–B5	1.720(7)	B12–H12	1.036(35)
B1–B4	1.732(7)	B4–C9	1.721(6)	B12–H1112	1.281(40)
B1–B5	1.723(8)	B4–C10	1.705(7)	C7–C8	1.534(5)
B1–B6	1.765(7)	B4–H4	1.045(38)	C7–H7a	1.012(29)
B1–H1	1.094(32)	B5–B6	1.738(7)	C7–H7b	1.046(38)
B2–B3	1.782(6)	B5–B11	1.749(7)	C8–C9	1.488(5)
B2–B6	1.755(7)	B5–C10	1.676(5)	C8–CA	1.498(5)
B2–B12	1.978(7)	B5–H5	1.044(37)	C9–C10	1.533(6)
B2–C7	2.236(6)	B6–B11	1.806(7)	C9–H9	1.018(27)
B2–C8	2.079(5)	B6–B12	1.800(7)	C10–H10	0.893(30)
B2–H2	1.133(35)	B6–H6	1.143(29)	CA–OA	1.334(5)
B3–B4	1.770(7)	B11–B12	1.897(8)	CA–OB	1.192(4)
B3–C8	1.679(5)	B11–C10	1.626(6)	CB–OA	1.463(5)
B3–C9	1.800(6)	B11–H11	1.074(36)	CB–HCBa	0.826(43)
B3–H3	1.089(30)	B11–H1112	1.259(43)	CB–HCBb	1.088(52)
		B12–C7	1.602(6)	CB–HCBc	0.966(32)

Table XI. Selected Bond Distances (Å) in PPN^+*arachno*-8-(NC)-7,8-$C_2B_{10}H_{14}^-$, **7**

B1–B2	1.687(10)	B12–C7	1.579(9)	B1–B3	1.738(9)
C7–C8	1.504(9)	B1–B4	1.768(7)	C8–CA	1.455(7)
B1–B5	1.713(7)	B2–B3	1.691(11)	B2–B6	1.825(10)
B2–B12	2.109(10)	B2–C8	1.899(7)	B3–B4	1.749(8)
B3–B9	1.813(6)	B3–C8	1.657(8)	B4–B5	1.734(9)
B4–B9	1.761(8)	B4–B10	1.708(9)	B5–B6	1.749(8)
B5–B10	1.700(7)	B5–B11	1.718(9)	B6–B11	1.779(6)
B6–B12	1.799(8)	B9–B10	1.840(9)	B9–C8	1.649(7)
B10–B11	1.809(10)	B11–B12	1.820(8)	CA–N1	1.144(7)
B1–B6	1.757(10)	B2–C7	2.173(9)		

These distances suggest a reduced bonding interaction between C6 and B2 and largely localized two-center single bonds between the C6 carbon and C5 and C7. Thus, the cluster could be considered to be composed of both "classical" electron-precise and "nonclassical" electron-deficient components. In the limit where C6 and B2 are nonbonding, then, instead of being considered part of the cluster framework, C6 might be viewed as a carbon–carbon bridging exopolyhedral substituent on the starting carborane framework, i.e. *arachno*-$\mu_{6,8}$-RCH-6,8-$C_2B_7H_{11}$. We have

Table XII. Selected Bond Distances (Å) in PPN$^+$*nido*-7-(MeC(O))-7,8-$C_2B_9H_{11}^-$, **8**

C7–CB8	1.570(4)	B5–H5	1.157(25)	B6–B10	1.766(4)
C7–B2	1.712(4)	B6–BC11	1.752(5)	C7–BC11	1.632(4)
B6–H6	1.091(25)	C7–B3	1.715(5)	B9–B10	1.808(5)
CB8–B4	1.690(5)	B9–H9	1.137(27)	CB8–B9	1.614(5)
B10–BC11	1.808(5)	CB8–B3	1.688(5)	B10–H10a	1.166(32)
CB8–H8	1.044(29)	B10–H10b	1.190(29)	C12–O1	1.216(4)
BC11–H11	1.313(31)	B1–B2	1.739(5)	B3–H3	0.985(35)
B1–B4	1.758(4)	B12–H10b	0.757(36)	B1–B5	1.793(5)
B1–B6	1.768(5)	B1–B3	1.731(5)	B1–H1	1.054(25)
B2–B6	1.748(5)	B2–BC11	1.763(5)	B2–B3	1.753(5)
B2–H2	1.171(24)	B4–B5	1.755(5)	B4–B9	1.797(6)
B4–B3	1.708(5)	B4–H4	1.135(40)	B5–B6	1.789(5)
B5–B9	1.759(5)	B5–B10	1.771(6)	C12–C13	1.459(5)
C7–C12	1.464(4)	C7–B12	1.543(17)	B9–B12	1.774(19)
B10–B12	1.819(17)	CB8–B12	1.632(20)	BC11–B12	1.647(17)

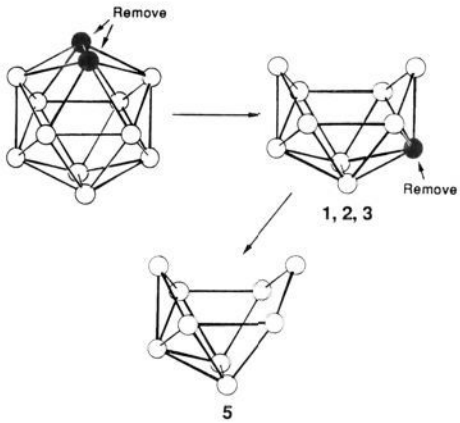

Figure 2. Derivation of the observed cage structures of *arachno*-6-(RCH_2)-5,6,7-$C_3B_7H_{12}$ (R = CN (**1**), C(O)OMe (**2**), or C(O)Me (**3**)) and *hypho*-1-($NCCH_2$)-1,2,5-$C_3B_6H_{12}^-$ (**5**) from an icosahedron.

previously discussed[12] similar structural features and alternative bonding descriptions for the related hybrid 9-vertex compounds *hypho*-1-CH_2-2,5-$S_2B_6H_8$ and *hypho*-1-BH_2-2,5-$S_2B_6H_9$.

The spectral data for compounds **1-3** are consistent with the solid-state structures determined for **1** and **2**. Thus, the infrared spectra contain absorptions characteristic of the –CN, –C(O)-Me, or –C(O)OMe groups and show no evidence of a carbon–carbon multiple bond. The ^{11}B NMR spectra for the three compounds show identical features, as shown in Figure 3b for **1**, consisting of 5 doublets in a ratio of 1:2:2:1:1, indicating C_s symmetry. In each spectrum, the intensity-two resonance near –4 ppm exhibits doublet fine structure characteristic of bridge-hydrogen coupling, leading to its assignment to the B8,10 borons. This assignment, as well as the other assignments in Table I, are consistent with a 2-D ^{11}B–^{11}B NMR experiment on compound **1**, where all expected crosspeaks were observed.

The proton-coupled ^{13}C NMR spectrum for each compound shows, in addition to the nitrile or methyl carbons, two doublets for the cage carbons in a ratio of 1:2 and a triplet for the CH_2 carbon. In the proton-decoupled ^{13}C NMR spectra, the intensity-two cage-carbon resonance shows multiplet structure consistent with coupling of the C5,7 carbons to the cage borons ($J_{^{11}B^{13}C}$ = ~35 Hz). The boron-11 decoupled ^{1}H NMR spectra revealed terminal BH, CH bridging hydrogens and two different cage CH protons in a ratio of 1:2. The resonances observed near 2.8 ppm in each compound are assigned to the methylene protons, which appear as doublets due to their coupling to the C6–H proton. The remaining assignments for the ^{1}H resonances in Table I were made on the basis of selective-decoupling experiments on **1**.

(12) (a) Kang, S. O.; Sneddon, L. G. *J. Am. Chem. Soc.* **1989**, *111*, 3281–3289. (b) Kang, S. O.; Sneddon, L. G. In *Electron Deficient Boron and Carbon Clusters;* Olah, G. A., Wade, K., Williams, R. E., Eds., Wiley: New York, 1991; pp 195–213.

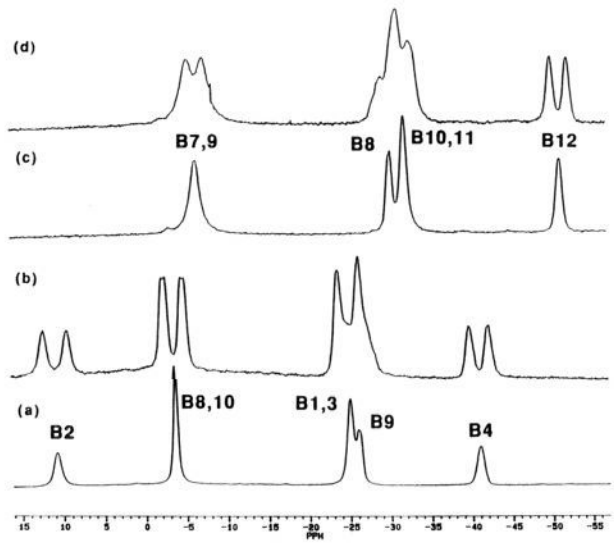

Figure 3. ^{11}B NMR spectra of (a) proton spin decoupled and (b) proton coupled *arachno*-6-($NCCH_2$)-5,6,7-$C_3B_7H_{12}$ (**1**) and (c) proton spin decoupled and (d) proton coupled *hypho*-1-($NCCH_2$)-1,2,5-$C_3B_6H_{12}^-$ (**5**).

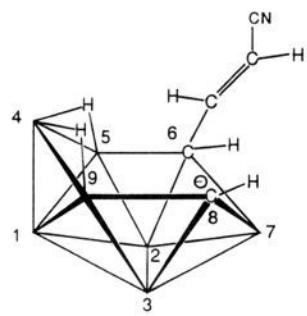

Figure 4. Proposed structure of *arachno*-6-(NCCH=CH)-6,8-$C_2B_7H_{11}^-$, **4**.

When the reaction of *arachno*-6,8-$C_2B_7H_{12}^-$ with cyanoacetylene was stopped before acidification, **4** was produced.

arachno-6,8-$C_2B_7H_{12}^-$ + NC≡CH →

arachno-6-(NCC(H)=CH)-6,8-$C_2B_7H_{11}^-$ (4)

The anion was isolated as its air-sensitive tetramethylammonium salt, the composition of which was established by elemental analysis. The structure proposed in Figure 4 containing a carbon-bound cyanovinyl substituent is supported by both the ^{1}H NMR spectrum, which shows complex vinyl-proton resonances in the 4–5 ppm region, and the infrared spectrum, which shows an absorption characteristic of a carbon–carbon double bond stretch at 1578 cm^{-1} and both cage and vinyl CH stretching bands in the 3000–3060 cm^{-1} region. The ^{11}B NMR spectrum, Table I, exhibits seven doublets, consistent with C_1 symmetry, with the absence of a singlet resonance supporting a carbon-substituted cyanovinyl group. The observed fine coupling ($J_{BH(br)}$ = 30 Hz) on the resonance at –16.9 ppm supports the presence of bridging hydrogens. It should also be noted that the chemical shifts of the boron resonances in **4** are in the ranges observed for the *arachno*-6,8-$C_2B_7H_{12}^-$ anion,[13] but they are very different than those observed for the isomeric tricarbaborane anion **1**$^-$ discussed below.

When anion **4** was acidified with anhydrous DCl, a deuterium-substituted tricarbaborane was obtained in 63% yield.

arachno-6-(NCC(H)=CH)-6,8-$C_2B_7H_{11}^-$ + DCl →

arachno-6-(NCCDH)-5,6,7-$C_3B_7H_{12}$ (5)

(13) Bausch, J. W.; Barnum, B. A.; Sneddon, L. G. Unpublished results.

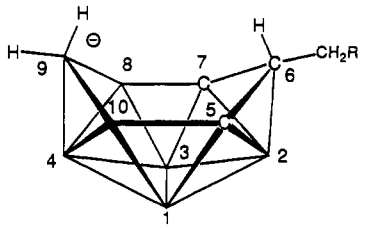

Figure 5. Proposed structure of *arachno*-6-$(NCCH_2)$-5,6,7-$C_3B_7H_{11}^-$, **1**$^-$.

The proton-decoupled ^{13}C spectrum of **1**-d_1, contains a 1:1:1 triplet (–C(D)H, J_{CD} = 21 Hz) at 26.6 ppm for the methylene carbon, indicating deuterium incorporation at this carbon, i.e. (NCC(D)H)-5,6,7-$C_3B_7H_{12}$. Likewise, the triplet C6–H resonance at –0.11 ppm in the ^1H NMR spectrum of **1** collapses to a doublet in **1**-d_1 due to coupling with only the single proton remaining on the –C(D)H group.

Deprotonation of **1** with KH in THF gave the monoanion, *arachno*-6-$(NCCH_2)$-5,6,7-$C_3B_7H_{11}^-$ (**1**$^-$). The anion was readily reprotonated by neutral water to yield **1**. **1**$^-$ is an isomer of **4**, but the spectral data for the two anions are very different, leading to the conclusion that they are of different structural types.

$$\textit{arachno}\text{-6-}(NCCH_2)\text{-5,6,7-}C_3B_7H_{12} + KH \rightarrow \textit{arachno}\text{-6-}(NCCH_2)\text{-5,6,7-}C_3B_7H_{11}^- + H_2 \quad (6)$$

The NMR data for **1**$^-$ support the symmetrical tricarbaborane structure shown in Figure 5. The ^{11}B NMR spectrum is consistent with C_s cage symmetry, and the presence of a BH_2 group is indicated by the intensity-one triplet resonance at –25.7 ppm. Therefore, the deprotonation of **1** results in both the loss of one bridge hydrogen and the conversion of the remaining bridging hydrogen to a terminal hydrogen on the B9 boron. Similar unbridged BH_2 groups have been found in other borane or carborane anions, including *nido*-3,4-Et_2-3,4-$C_2B_5H_6^-$,[14] *nido*-$B_{11}H_{14}^-$,[15] and *nido*-7,8-$C_2B_9H_{12}^-$.[16] The *endo*-B9H resonance appears as a quartet at –3.06 ppm in the ^1H NMR spectrum, and both its shift and the magnitude of the B–H coupling (J_{BH} = 70 Hz) are similar to that observed for the *endo* proton in *nido*-3,4-Et_2-3,4-$C_2B_5H_6^-$. The proton NMR spectrum also shows two cage CH resonances at 0.67 and 0.31 ppm, respectively, in a 2:1 ratio. The ^1H NMR assignments shown in Table I are again consistent with selective-decoupling experiments.

Generally, it has been found that one proton on a cage CH_2 group, as in for example *arachno*-6,8-$C_2B_7H_{13}$, is more acidic than a bridging hydrogen.[17] The fact that in **1** a bridging hydrogen is more acidic than the –CH_2 protons provides additional chemical evidence for the "classical" nature of the C6 carbon.

Compound **1** reacted readily with ammonium hydroxide to give the new tricarbaborane *hypho*-1-$(NCCH_2)$-1,2,5-$C_3B_6H_{12}^-$ (**5**) as the only cage degradation product.

$$\textit{arachno}\text{-6-}(NCCH_2)\text{-5,6,7-}C_3B_7H_{12} \xrightarrow{NH_4OH} \textit{hypho}\text{-1-}(NCCH_2)\text{-1,2,5-}C_3B_6H_{12}^- \quad (7)$$

A single-crystal X-ray study has confirmed the structure shown in the ORTEP drawing in Figure 6. The observed cage structure may be derived from that found for **1** by removal of the B2 framework atom of **1**. As a result, a new five-membered open face containing the C1–C2–B11–B10–C5 atoms is generated which contains a single bridging hydrogen on the B10–B11 edge. Two other bridging hydrogens are present at the B7–B8 and B8–B9 edges in the puckered six-membered open face. Examination of the interatomic distances and angles shows that the C1 atom is in a nearly tetrahedral environment: C5–C1–C13 (109.9(2)°), C2–C1–C13 (110.4(2)°), and C5–C1–C2 (109.8(2)°). The C1–C2 (1.531(3) Å) and C1–C5 (1.539(3) Å) distances are again in the range expected for normal carbon-carbon single bonds (for example, C1–C13 = 1.537(3) Å), but they are somewhat shorter than the carbon–carbon distances in **1**. Relatively long distances are found between B9–B10 and B7–B11, 1.943(6) and 1.921(5) Å, respectively. In **1** and **2**, the pentagonal ring containing the three carbons (C5, C6, C7, B1, and B3) is planar, but in **5** the methylene carbon C1 is distorted ~0.38 Å out of the C2,C5,B10,B11 plane. The overall cage geometry is, in fact, quite similar to that previously confirmed[12] for *hypho*-1-(CH_2)-2,5-$S_2B_6H_8$, which contains a methylene group bridging the two sulfur cage atoms. The remaining bond distances and angles in the cage are within the normal ranges expected for carboranes.

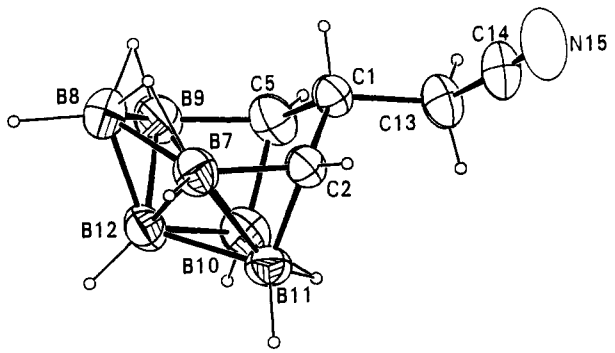

Figure 6. ORTEP drawing of the cage structure of *hypho*-1-$(NCCH_2)$-1,2,5-$C_3B_6H_{12}^-$, **5**.

There are at least two different ways in which the structure of **5** can be viewed. First, if the anion is considered a tricarbaborane cluster, then the compound would contain 26 electrons and fall into the 9-vertex $2n + 8$ hypho electronic class (n = number of cage atoms) and should adopt a structure based on an icosahedron missing three vertices. Such cage geometries have been observed for the isoelectronic analogues *hypho*-1-(CH_2)-2,5-$S_2B_6H_8$[12] and *hypho*-1,2,5-(η^6-C_6Me_6)$RuClS_2B_6H_9$[18] and may be derived in a straightforward manner for **5**, as illustrated in Figure 2.

Alternatively, the $(NCCH_2)CH$– group may be viewed as an *exo*-polyhedral substitutent on a C_2B_6 cluster, i.e. *hypho*-$\mu_{2,5}$-$(NCCH_2)CH$-2,5-$C_2B_6H_{11}^-$. As for *hypho*-1-(CH_2)-2,5-$S_2B_6H_8$ (*exo*-CH_2 substituent)[12] and *hypho*-1,2,5-(η^6-C_6Me_6)$RuClS_2B_6H_9$ (*exo*-(η^6-C_6Me_6)RuCl substituent),[18] the $(NCCH_2)CH$– fragment could then be considered to bond to the two cage carbons by two conventional 2-center, 2-electron bonds. The tetrahedral angles at C1 and the C1–C2 and C1–C5 bond distances support this interpretation. In this view, **5** would be considered a carbon-bridged derivative of the previously known[19] dicarbaborane anion *hypho*-7,8-$C_2B_6H_{13}^-$, in which two *endo* hydrogens are replaced by the carbon-bridging $(NCCH_2)CH$– group.

The spectroscopic data for **5** are again in accord with the solid-state structure. The ^{11}B NMR spectrum, as shown in Figure 3d, is similar to that of **1**, Figure 3b, with the exception that, as expected, the low-field resonance assigned to the B2 boron in **1** is missing in **5**. All expected crosspeaks were observed in a ^{11}B–^{11}B COSY experiment. The observed shifts and the assignments are, in fact, quite similar to those observed[19] for *hypho*-7,8-$C_2B_6H_{13}^-$ (–5.71 ppm, B2,5; –31.39 ppm, B6; –33.25 ppm, B3,4;

(14) (a) Beck, J. S.; Quintana, W.; Sneddon, L. G. *Organometallics* **1988**, *7*, 1015–1016. (b) Beck, J. S.; Sneddon, L. G. *Inorg. Chem.* **1990**, *29*, 295–302.

(15) Getman, T. D.; Krause, J. A.; Shore, S. G. *Inorg. Chem.* **1988**, *27*, 2398–2399.

(16) (a) Buchanan, J.; Hamilton, E. J. M.; Reed, D.; Welch, A. J. *J. Chem. Soc., Dalton Trans.* **1990**, 677–680. (b) Fontaine, X. L. R.; Greenwood, N. N.; Kennedy, J. D.; Nestor, K.; Thornton-Pett, M.; Heřmánek, S.; Jelinek, T.; Štíbr, B. *J. Chem. Soc., Dalton Trans.* **1990**, 681–689.

(17) Williams, R. *Adv. Inorg. Chem. Radiochem.* **1976**, *18*, 67–142.

(18) Mazighi, K.; Carroll, P. J.; Sneddon, L. G. *Inorg. Chem.* **1992**, *31*, 3197-3204.

(19) Jelinek, T.; Plešek, J.; Heřmánek, S.; Štíbr, B. *Main Group Met. Chem.* **1987**, *10*, 387–388.

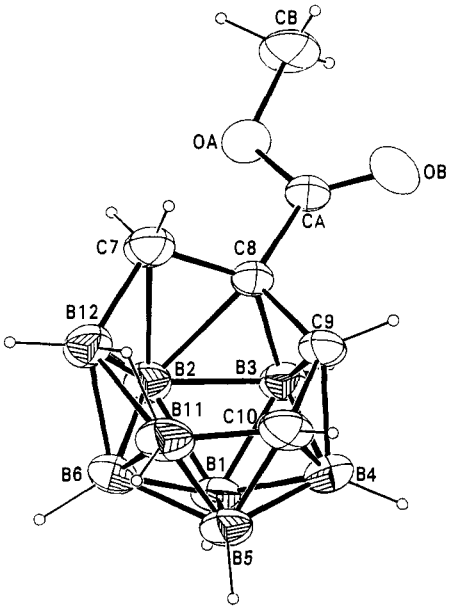

Figure 7. ORTEP drawing of the structure of *arachno*-8-($CH_3OC(O)$)-7,8,9,10-$C_4B_8H_{13}$, **6**.

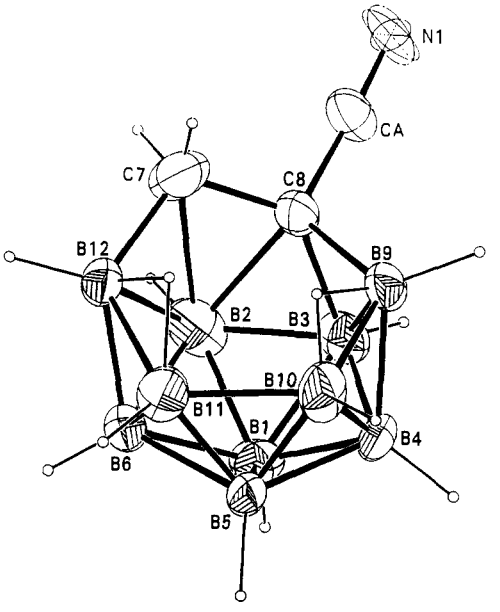

Figure 8. ORTEP drawing of the cage structure of *arachno*-8-(NC)-7,8-$C_2B_{10}H_{14}^-$, **7**.

−55.34 ppm, B1). Two types of bridging hydrogens with an intensity ratio of 2:1 were observed in the boron-decoupled ^1H NMR spectrum. The B10–H–B11 bridging hydrogen at −3.01 ppm appears as a triplet due to its coupling to H11 and H10. All terminal hydrogens were found, and their assignments were established by selective proton-decoupling experiments. In addition to the cyano–carbon resonance, the ^{13}C NMR spectrum showed one broad doublet, one sharp doublet, and one triplet arising from the C2,5, C1, and C13 carbons, respectively.

Dicarbon Insertion Reactions: Syntheses of Di- and Tetracarbon Carboranes. *arachno*-8-($CH_3OC(O)$)-7,8,9,10-$C_4B_8H_{13}$ (6) and *arachno*-8-(NC)-7,8-$C_2B_{10}H_{14}^-$ (7). The *nido*-5,6-$C_2B_8H_{11}^-$ anion reacted smoothly with methyl propiolate in THF to give intermediate anions which, upon acidification, converted to *arachno*-8-($CH_3OC(O)$)-7,8,9,10-$C_4B_8H_{13}$. The new tetracarbaborane was isolated in 57% yield as a white air-sensitive solid. The compound can be stored in vacuo at 0 °C without decomposition. Further purification can be achieved by recrystallization from cold pentane.

$$nido\text{-}5,6\text{-}C_2B_8H_{11}^- + HC{\equiv}CC(O)OMe \xrightarrow[(2)\ H^+]{(1)\ RT}$$

$$arachno\text{-}8\text{-}(CH_3OC(O))\text{-}7,8,9,10\text{-}C_4B_8H_{13} \quad (8)$$

The composition of the product was initially established by both elemental analysis and exact mass measurements. As shown in the ORTEP drawing in Figure 7, the crystallographically established structure confirms that two-carbon insertion of the methyl propiolate acetylenic carbons into the carborane framework has occurred to produce a tetracarbaborane. The terminal acetylenic carbon is present (C7) as a CH_2 group, and the ester group is bound to C8. The C7–C8 1.534(5)-Å and B12–C7 1.602-(6)-Å distances are in the normal range for intracage C–C and B–C distances. The cage contains a puckered six-membered open face composed of the C7, C8, C9, C10, B11, and B12 atoms with the four cage carbons in adjacent positions and a single bridging hydrogen present at the B11–B12 edge. The C8, C9, C10, B11, and B12 atoms form a plane parallel to the B2–B3–B4–B5–B6 plane. C7 is distorted out of the C8–C9–C10–B11–B12 plane by 0.63 Å. The B2 cage atom is formally six-coordinate being connected to the C7–C8–B3–B1–B6–B12 ring. The C8–B12–B6–B1–B3 atoms are planar, but the C7 atom is distorted out of this plane by ~0.3 Å toward the B2 atom. The B2 atom occupies an asymmetric position above the ring (B2-ring-centroid 0.87 Å), with long distances being observed to B12, C7, and C8 (B2–B12 = 1.978(7) Å, C7–B2 = 2.236(6) Å, and B2–C8 = 2.079(5) Å), suggesting weak interactions with these atoms. The C7–B2 distance is, in fact, longer that those between C6 and B2 in **1** and **2**, again suggesting that the primary bonding interaction of the C7 carbon in **6** is with C8 and B12. The remaining intracage distances are within the ranges expected for carboranes.

The spectroscopic data are consistent with the established solid-state structure. The ^{11}B NMR spectrum exhibits eight doublets of equal intensity indicating C_1 cage symmetry. The resonance at −26.0 ppm (J_{BH} = 140 Hz, $J_{BH(br)}$ = 64 Hz) exhibits a doublet-of-doublets structure indicative of bridge-hydrogen coupling. The ^1H NMR spectrum exhibits four CH resonances with the peaks at 1.47 and 1.06 ppm appearing as a doublet and triplet, respectively, leading to their assignments to the protons on the $-CH_2$ group. All terminal −BH protons and a single bridging-proton resonance were located in the ^{11}B-decoupled proton NMR spectrum. Selective proton-decoupling experiments showed that the bridging hydrogen was strongly coupled to one terminal BH and to the CH resonance at 1.06 ppm, supporting the assignment of the latter peak to the *endo*-C7H proton. In addition to the resonances arising from the carbonyl and methyl groups, the proton-coupled room temperature ^{13}C NMR spectrum showed one singlet, two doublets, and one triplet resonances for the cage carbons, with the latter signal assigned to the CH_2 carbon.

The reaction of *nido*-$B_{10}H_{13}^-$ with cyanoacetylene in THF solution produced a new dicarbaborane anion, *arachno*-8-(NC)-7,8-$C_2B_{10}H_{14}^-$. Addition of PPN^+Cl^- to the reaction solution led to the isolation of its air-stable crystalline PPN^+ salt in 87% yield, the composition of which was established by elemental analysis. The anion did not react upon treatment with HCl·diethyl ether.

$$nido\text{-}B_{10}H_{13}^- + HC{\equiv}CCN \rightarrow$$

$$arachno\text{-}8\text{-}(NC)\text{-}7,8\text{-}C_2B_{10}H_{14}^- \quad (9)$$

The *arachno*-8-(NC)-7,8-$C_2B_{10}H_{14}^-$ is isoelectronic with **6** and a similar cage structure would be expected. Indeed, as shown in the ORTEP drawing in Figure 8, the gross cage structure is identical with that observed for *arachno*-8-($CH_3OC(O)$)-7,8,9,-10-$C_4B_8H_{13}$. The cyano substituent is attached to C8, thus the C7 and C8 cage atoms are readily identified as the acetylenic carbons. The two carbon atoms remain adjacent in the six-membered open face composed of the C7–C8–B9–B10–B11–

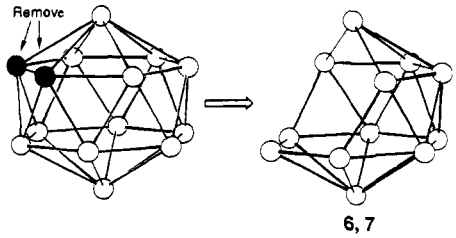

Figure 9. Derivation of the observed cage structures of *arachno*-8-$(CH_3OC(O))$-7,8,9,10-$C_4B_8H_{13}$ (**6**) and *arachno*-8-(NC)-7,8-$C_2B_{10}H_{14}^-$ (**7**) from a bicapped hexagonal antiprism.

B12 atoms. As in **6**, C7 is distorted out of the C8–B9–B10–B11–B12 plane by 0.60 Å. The C7–C8 distance 1.504(9) Å again indicates reduction of the acetylenic bond. The B2 cage atom is formally six-coordinate, being connected to the C7–C8–B3–B1–B6–B12 ring. Again, as in **6**, the C8–B3–B1–B6–B12 atoms form a plane, and the C7 atom is distorted out of this plane by ~0.24 Å toward the B2 atom. The B2 atom also occupies an asymmetric position above the ring (B2 ring centroid, 0.90 Å), with long distances being observed to B12, C7, and C8 (B2–B12 = 2.109(10) Å, C7–B2 = 2.173(9) Å, and B2–C8 = 1.899(7) Å). The CA–N1 distance, 1.144(7) Å, is similar to that found in *arachno*-6-$(NCCH_2)$-5,6,7-$C_3B_7H_{12}$ (1.145(7) Å), and the C8–CA–N1 angle is approximately linear, 177.6(4)°. The remaining cage distances and angles are normal.

The spectroscopic data are consistent with the above structure. The ^{11}B NMR spectrum at 160.5 MHz shows 9 doublets with the intensity-2 resonance at –6.2 ppm arising from the overlap of two signals. The ^{11}B-decoupled ^1H NMR spectrum shows all expected terminal BH and two CH resonances, in addition to the two bridging-hydrogen resonances centered at –1.93 and –3.95 ppm. Two doublet-of-doublets signals, arising from the *endo*-C7H and *exo*-C7H protons, were found at 0.68 and 1.14 ppm, respectively. Selective proton-decoupling experiments showed that the CH proton at 0.68 ppm is strongly coupled to the bridging hydrogen at –1.93 ppm, but not to the one at –3.95 ppm, leading to its assignment to the *endo*-C7H and the resonances at –1.93 and –3.95 ppm to the B11–H–B12 and B9–H–B10 protons, respectively. The doublet-of-doublets structure of the *exo*-C7H was found to result from its coupling to both the *endo*-C7H proton and the terminal B12H proton at 2.51 ppm. The room temperature proton-coupled ^{13}C NMR spectrum showed, in addition to the nitrile carbon signal, a broad singlet at 3.37 ppm and a broad triplet at –4.59 ppm (J_{CH} = 137 Hz) arising from the C8 and C7 cage carbons, respectively.

As for **1-3** and **5**, the structures of **6** and **7** can be described in two ways. If they are considered as 12-vertex clusters, then on the basis of their 30 skeletal-electron counts, they would be considered *arachno* cage systems and, therefore, should adopt cage geometries derived from a bicapped hexagonal antiprism missing two vertices. Indeed, as demonstrated in Figure 9, the observed structures can be derived in this manner by removing a pair of adjacent five-connected vertices. The observed structures for **6** and **7** are consistent with that found for the first structurally characterized 12-vertex *arachno* cluster, $[\sigma$-$(\eta^5$-$C_5H_5)Co(\eta^4$-$C_5H_4)^+]$-$(CH_3)_4$-*arachno*-$C_4B_8H_8^-$.[20]

Alternatively, because of the weak interaction between B2 and C7 in **6** (2.236(6) Å) and **7** (2.173(9) Å), both compounds can be viewed as 11-vertex *arachno* cage systems containing exopolyhedral methylene groups bridging the C8 and B12 cage atoms. This view is supported by the near tetrahedral geometry about C7. For example, the bond angles for B12–C7–C8, H7a–C7–C8, and H7b–C7–C8 in **6** are 108.9(3)°, 104.4(17)°, and 103.5(21)°, respectively. In the limit that C7–B2 has no bonding interaction, then a four membered open face composed of the C7–B12–B2–C8 atoms would result. Likewise, the cage structure observed for $[\sigma$-$(\eta^5$-$C_5H_5)Co(\eta^4$-$C_5H_4)^+]$-$(CH_3)_4$-*arachno*-$C_4B_8H_8^-$ could be alternatively described as an 11-vertex cluster containing a cobaltocenium-substituted exopolyhedral bridging methylene, μ-$CH[(\eta^5$-$C_5H_5)Co(\eta^4$-$C_5H_4)^+]$-*arachno*-$C_3B_8H_7^-$.

The structures of **6** and **7** may be compared with those observed for other 12-vertex *nido*-carboranes. The observed structures are quite different than those observed in the solid state for *nido*-$Me_4C_4B_8H_8$ and *nido*-$Et_4C_4B_8H_8$, which are composed of a distorted icosahedral cage containing two quadrilateral open faces, and two pyramidal C_2B_4 units joined at their basal B–B edges, respectively.[21] Two cage isomers of *nido*-$R_2C_2B_{10}H_{11}^-$ have previously been characterized.[22,23] Studies of the thermodynamic or "stable" isomer *nido*-$R_2C_2B_{10}H_{11}^-$ (R = Ph[24] and Me[25]) have shown that this isomer has a cage geometry based on a monocarbon 11-vertex nido cage fragment containing a boron–boron bridging-methylene group (–C(Me)H and –C(Ph)H, respectively) on the open face. Recently, a structural study of the kinetic or "unstable" isomer $[PPh_3Me^+][$*nido*-7,9-$Me_2C_2B_{10}H_{11}^-]$ has confirmed a different cage geometry based on a 12-vertex *nido* fragment that may be obtained by the removal of the hexagonal vertex from the parent 13-vertex *closo*-docosahedral polyhedron.[26] In this isomer, both carbons have only one bound hydrogen, with one carbon bound to three cage boron atoms (<1.8 Å), which results in a quadrilateral opening in the structure. The structures observed for **6** and **7** appear more closely related to that observed for the "unstable" isomer; however, in **6** and **7**, the methylenes, $-CH_2$ (C7), are within normal bonding distance to only C8 and B12 with the C7–B2 distance being quite long, creating an apparent quadrilateral face. Long distances are also found in the four-membered open face for B2–B12 (1.978(7) Å, **6**; 2.109(10) Å, **7**) and B2–C8 (2.079(5) Å, **6**; 1.899(7) Å, **7**). A similar type of quadrilateral distortion was observed in σ-$(\eta^5$-$C_5H_5)Co(\eta^4$-$C_5H_4)^+$-$(CH_3)_4C_4B_8H_8^-$.[20] These differences in the structures of the 12-vertex *nido* and *arachno* cage geometries are, of course, consistent with the fact that addition of electrons to the cluster framework should result in a more open cage.

***nido*-7-(RC(O))-7,8-$C_2B_9H_{11}^-$ (R = Me (8) or OMe (9)).** In contrast to the reaction of *nido*-$B_{10}H_{13}^-$ with cyanoacetylene, which produces the 12-vertex *arachno*-dicarbaborane **7**, the reaction of *nido*-$B_{10}H_{13}^-$ with 2 equiv of either 3-butyn-2-one or methyl propiolate results in the formation of the 11-vertex *nido*-dicarbaboranes, *nido*-7-(RC(O))-7,8-$C_2B_9H_{11}^-$ (R = Me (**8**) or OMe (**9**)). The anions were isolated in ~75% yields as their air stable crystalline tetramethylammonium or PPN^+ salts. The compositions of both compounds were established by elemental analyses.

$$\textit{nido}\text{-}B_{10}H_{13}^- + HC{\equiv}CC(O)R \rightarrow \textit{nido}\text{-}7\text{-}(RC(O))\text{-}7,8\text{-}C_2B_9H_{11}^- \quad (10)$$

R = Me (**8**) or OMe (**9**)

In both reactions, 2 equiv of the acetylenes were necessary; since when only 1 equiv was used, a mixture of equal amounts of *nido*-7-(RC(O))-7,8-$C_2B_9H_{11}^-$ and unreacted *nido*-$B_{10}H_{13}^-$ (estimated by ^{11}B NMR) was obtained. Lowering the reaction

(20) Grimes, R. N.; Pipal, J. R.; Sinn, E. *J. Am. Chem. Soc.* **1979**, *101*, 4172–4180.

(21) (a) Freyberg, D. P.; Weiss, R.; Grimes, R. N.; Sinn, E. *Inorg. Chem.* **1977**, *16*, 1847–1851. (b) Venable, T. L.; Maynard, R. B.; Grimes, R. N. *J. Am. Chem. Soc.* **1984**, *106*, 6187–93. (c) Grimes, R. N. *Adv. Inorg. Chem. Radiochem.* **1983**, *26*, 55–116 and references therein.

(22) (a) Dunks, G. B.; Wiersema, R. J.; Hawthorne, M. F. *J. Chem. Soc., Chem. Commun.* **1972**, 899–900. (b) Dunks, G. B.; Wiersema, R. J.; Hawthorne, M. F. *J. Am. Chem. Soc.* **1973**, *95*, 3174–3179.

(23) A computational study of these two isomers has recently been reported, see: McKee, M. L.; Bühl, M.; Schleyer, P. v. R. *Inorg. Chem.* **1993**, *32*, 1712–1715.

(24) (a) Tolpin, E. I.; Lipscomb, W. N. *J. Chem. Soc., Chem. Commun.* **1973**, 257–258. (b) Tolpin, E. I.; Lipscomb, W. N. *Inorg. Chem.* **1973**, *12*, 2257–2262.

(25) Churchhill, M. R.; DeBoer, B. G. *Inorg. Chem.* **1973**, *12*, 2674–2682.

(26) Getman, T. D.; Knobler, C. B.; Hawthorne, F. M. *Inorg. Chem.* **1990**, *29*, 158–160.

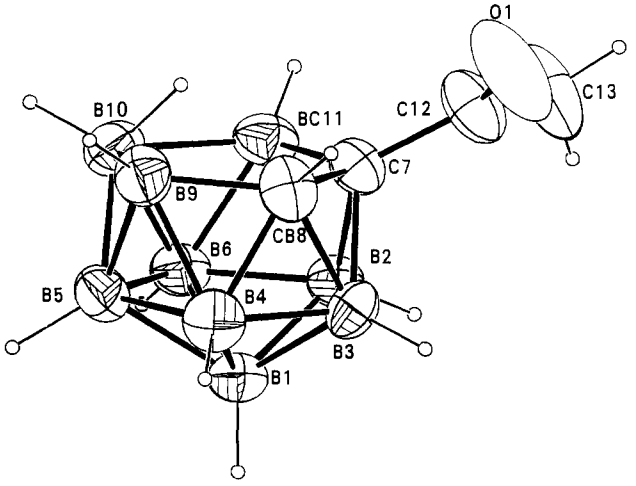

Figure 10. ORTEP drawing of the cage structure of *nido*-7-(MeC(O))-7,8-$C_2B_9H_{11}^-$, **8**.

temperature to 0 °C made little difference in the product distribution but gave a large decrease in the reaction rates.

A single-crystal X-ray study of **8**, as shown in the ORTEP drawing in Figure 10, established that **8** and **9** are carbon-substituted derivatives of the *nido*-7,8-$C_2B_9H_{12}^-$ cage system. In agreement with the recent X-ray crystallographic[16a] and NMR[16b] studies of 7,8-$C_2B_9H_{12}^-$, an *endo*-hydrogen was located at the B10 boron on the open face. Likewise, the boron–boron and carbon–boron intracage distances and angles are quite similar to those found for the parent 7,8-$C_2B_9H_{12}^-$.

The ^{11}B NMR spectra of **8** and **9** contain nine doublet resonances indicating C_1 cage symmetry. All terminal BH and a single cage–CH resonance were observed for both compounds in their ^{11}B-decoupled ^{1}H-NMR spectra. Both the ^{11}B and ^{1}H NMR spectra show evidence that the *endo*-B10H hydrogen observed in the solid-state structure may adopt a bridging position at the B10–B9 edge in solution. For example, in the ^{11}B NMR spectra, the peak near −31 ppm shows a doublet-of-doublets structure typical of a boron coupled to both a terminal (J_{BH} = ~135 Hz) and one bridging hydrogen ($J_{BH(br)}$ = ~40 Hz). Likewise, the ^{1}H NMR spectra of **8** and **9** show broad resonances near −2.6 ppm with line widths typical of bridge hydrogens. In addition to the resonance resulting from the carbonyl carbons, the ^{13}C NMR spectra of **8** and **9** show one broad singlet and one broad doublet resonance arising from the C7 and C8 carbons.

***arachno*-[*endo*-4-(NCCH=CH)]-6,8-$S_2B_7H_8^-$ (10).** The thiaborane anion, *arachno*-6,8-$S_2B_7H_8^-$, readily reacts with cyanoacetylene at room temperature to give one product, *arachno*-[*endo*-4-(NCCH=CH)]-6,8-$S_2B_7H_8^-$, which was isolated as its tetramethylammonium salt in 68% yield.

$$\textit{nido}\text{-}6,8\text{-}S_2B_7H_8^- + HC{\equiv}CCN \rightarrow$$

$$\textit{arachno}\text{-}[\textit{endo}\text{-}4\text{-}(NCCH{=}CH)]\text{-}6,8\text{-}S_2B_7H_8^- \quad (11)$$

The elemental analysis, spectroscopic data, and a single-crystal X-ray determination[27] are consistent with the formation of an *endo* B-substituted cyanovinyl group, *arachno*-[*endo*-4-(NCCH=CH)]-6,8-$S_2B_7H_8^-$, as depicted in Figure 11. The ^{11}B-NMR spectrum consists of 5 doublets in a ratio of 2:1:1:2:1, indicating C_s cage symmetry. Substitution at the B4 position is indicated, since in *arachno*-6,8-$S_2B_7H_8^-$ the B4 resonance occurs as a triplet at −50.8 ppm while in **10** this resonance is replaced by a doublet at −38.0 ppm. The proton-coupled ^{13}C NMR spectrum shows vinyl carbons at 92.0 (doublet) and 189.5 ppm (doublet-of-quartets), along with a multiplet at 122.8 ppm resulting from the nitrile carbon. In the proton-decoupled spectrum, a quartet ($J_{^{13}C^{11}B}$ = 62 Hz) centered at 189.5 ppm was

(27) Wille, A.; Su, K.; Carroll, P. J.; Sneddon, L. G. In preparation.

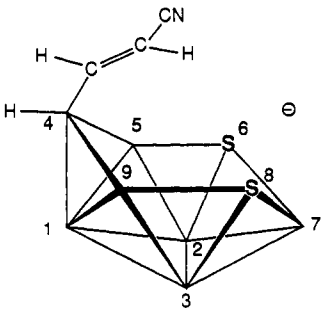

Figure 11. Established structure of *arachno*-[*endo*-4-(NCCH=CH)]-6,8-$S_2B_7H_8^-$, **10**.

observed, which at −85 °C collapsed (due to thermal decoupling of ^{11}B)[28] to a singlet, leading to its assignment to the olefinic carbon directly bonded to B4. The presence of the vinyl group is further supported by the ^{1}H NMR spectrum, which shows complex olefinic C–H resonances at 5.70 (doublet-of-doublets) and 4.87 (multiplet) ppm. The B4–H proton was found at 0.77 ppm, and selective ^{1}H-decoupling experiments confirmed that this proton was coupled to the C–H proton at 5.70 ppm. The C=C bond stretch (1528 cm^{-1}) in the infrared spectrum is lower than those of normal carbon–carbon double bonds[29] (1640–1667 cm^{-1}) due to conjugation with the cyano group, but it is higher than that in acrylonitrile[30] (1411 cm^{-1}). As expected, the nitrile band in **10** (2198 cm^{-1}) occurs at similar frequency as **4** (2198 cm^{-1}), but at a lower frequency than those observed in **1** (2248 cm^{-1}) or **5** (2234 cm^{-1}), where double bond conjugation is absent.

On the basis of the reaction in eq 3, it was expected that the reaction of **10** with acid should lead to carbon insertion products, but only decomposition was observed upon treatment with anhydrous HCl in CH_2Cl_2. The conversion of vinyl derivatives of other boranes and carboranes to carbon-insertion products has also been observed upon thermolysis;[31] however, heating neither *arachno*-[*endo*-4-(NCCH=CH)-6,8-$S_2B_7H_8^-$] at reflux in glyme, nor its tetramethylammonium salt as a solid at 160 °C resulted in such products.

Discussion

The results presented above have clearly demonstrated that terminal acetylenes containing strongly electron-withdrawing groups are activated toward reaction with various polyhedral borane anions and that such reactions can ultimately lead to monocarbon or dicarbon insertions. This reaction sequence has thus allowed the syntheses of several unique types of new carboranes. Of particular importance are the reactions leading to the tricarbaboranes **1**-**3** and **5** since, in contrast to the numerous dicarbaboranes, only a few tricarbaboranes, *nido*-2,3,4-$R_2C_3B_3H_5$.[32] *nido*-2,3,5-$R_5C_3B_3H$[33] (R = alkyl or H), *closo*-

(28) (a) Wrackmeyer, B. In *Progress in NMR Spectroscopy*, Emsley, J. W., Feeney, J., Sutcliffe, L. H., Eds.; Pergamon: New York, 1979; Vol. 12, pp 227–259. (b) Gragg, B. R.; Layton, W. J.; Niedenzu, K. *J. Organomet. Chem.* **1977**, *132*, 29–36.

(29) Silverstein, R. M.; Bassler, G. C.; Morrill, T. C. *Spectrometric Identification of Organic Compounds*; Wiley: New York, 1991, pp 105–106.

(30) *Raman/Infrared Atlas of Organic Compounds*; Schrader, B. Ed., VCH: New York, 1989, p C3–05.

(31) (a) Wilczynski, R.; Sneddon, L. G. *J. Am. Chem. Soc.* **1980**, *102*, 2857–2858. (b) Wilczynski, R.; Sneddon, L. G. *Inorg. Chem.* **1981**, *20*, 3955–3962.

(32) (a) Bramlett, C. L.; Grimes, R. N. *J. Am. Chem. Soc.* **1966**, *88*, 4269–4270. (b) Grimes, R. N.; Bramlett, C. L. *J. Am. Chem. Soc.* **1967**, *89*, 2557–2560. (c) Grimes, R. N.; Bramlett, C. L.; Vance, R. L. *Inorg. Chem.* **1968**, *7*, 1066–1070.

(33) (a) Kuhlmann, T.; Pritzkow, H.; Zenneck, U.; Siebert, W. *Angew. Chem., Int. Ed. Engl.* **1984**, *23*, 965–966. (b) Zwecker, J.; Pritzkow, H.; Zenneck, U.; Siebert, W. *Angew. Chem., Int. Ed. Engl.* **1986**, *25*, 1099–1100. (c) Zwecker, J.; Kuhlmann, T.; Pritzkow, H.; Siebert, W.; Zenneck, U. *Organometallics* **1988**, *7*, 2316–2324. (d) Siebert, W.; Schafer, V.; Brodt, G.; Fessenbecker, A.; Pritzkow, H. *Abstracts of Papers*, 200th ACS National Meeting, Washington, DC, August, 1990, paper No. INOR 381.

$C_3B_5H_7$,[34] *nido*-6-CH_3-5,6,9-$C_3B_7H_{10}^-$,[1,35] and *hypho*-$C_3B_4H_{12}$,[36] have previously been reported.[37] Thus, the chemistry of this cluster class has not been extensively developed. The *arachno*-6-(RCH_2)-5,6,7-$C_3B_7H_{12}$ carboranes **1-3** are the first examples of polyhedral tricarbaboranes in the *arachno* electronic class,[38] and **1**, **2**, and **5** are the first tricarbaboranes to be structurally characterized. Our initial investigations of the coordination chemistry of the *nido*-tricarbaborane monoanion *nido*-6-CH_3-5,6,9-$C_3B_7H_9^-$ have shown[35] that tricarbaborane anions exhibit a diverse organometallic chemistry with the resulting metallatricarbaboranes having properties that bridge the polyhedral borane, organometallic, and metal cluster areas. Both the mono- and trianions of the *arachno*-tricarbaboranes, i.e. *arachno*-6-(RCH_2)-5,6,7-$C_3B_7H_{11}^-$ and *arachno*-6-(RCH_2)-5,6,7-$C_3B_7H_9^{3-}$, should now be accessible, and this should result in a considerable expansion of the coordination chemistry and structural diversity of metallatricarbaborane clusters.

Likewise, the supraicosahedral clusters **6** and **7** resulting from the two carbon insertions into the $C_2B_8H_{11}^-$ and $B_{10}H_{13}^-$-frameworks are also unique. Although several 12-vertex *nido* clusters, including the tetracarbaboranes *nido*-R_4-2,3,7,8-$C_4B_8H_8$[21,39] and *nido*-2,7-$(Me_3Si)_2$-2,3,7,8-$C_4B_8H_{10}$[40] and the dicarbaborane anion *nido*-$R_2C_2B_{10}H_{11}^-$,[22-26] have been reported, only two 12-vertex *arachno* carborane clusters are known: σ-$(\eta^5$-$C_5H_5)Co(\eta^4$-$C_5H_4)^+$-$(CH_3)_4C_4B_8H_8^-$ and *arachno*-$(CH_3)_4$-$C_4B_8H_8^{2-}$.[20] Preliminary chemical studies of **6** and **7** have shown that these new carboranes can be used to generate a range of new supraicosahedral metallacarborane clusters.[41]

The reactions in eqs 8 and 9 resulted in the production of the previously unknown C-substituted ketone (**8**) and ester (**9**) dicarbollide derivatives, *nido*-7-R-7,8-$C_2B_9H_{11}^-$. Since the traditional routes to most intermediate dicarbaboranes, including the dicarbollide anion, have employed degradation reactions of either *ortho*- or *meta*-$C_2B_{10}H_{12}$,[42] the reactions of *nido*-$B_{10}H_{13}^-$ with methyl propiolate and 3-butyn-2-one provide a new alternative one-step pathway to the dicarbollides directly from decaborane(14).

Although the mechanisms of the insertion reactions have not yet been studied in detail, the results of previous studies[43] of the reactions of polarized acetylenes with organic nucleophiles, as well as the isolation of compounds **4** and **10**, suggest several steps in the reaction sequences that are important to both the monocarbon and dicarbon insertion reactions. The acetylenes, cyanoacetylene, methyl propiolate, and 3-butyn-2-one are strongly polarized by the cyano or carbonyl groups with the terminal carbons in each compound having a partial positive charge. As a result, these acetylenes undergo attack at the terminal carbons by organic nucleophiles, such as alcohols or mercaptans.[43a] Subsequent rearrangements in these organic systems can then lead to the incorporation of either one or two carbons into a ring system.

Scheme I. Possible Reaction Pathways Leading to (A) monocarbon (B) Dicarbon Insertion

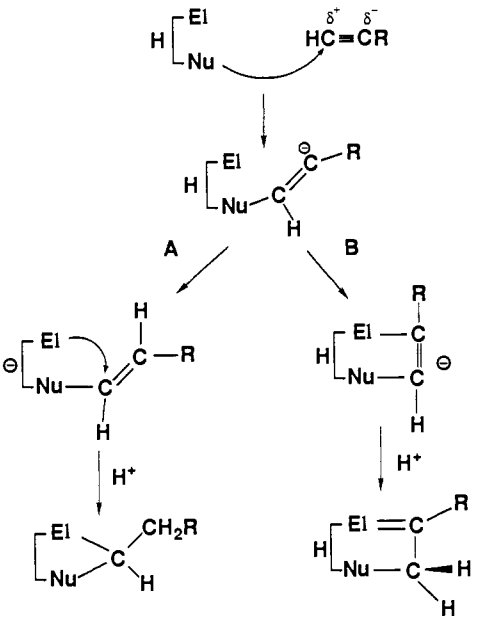

As shown in Scheme I, a reaction sequence based on those previously suggested[41a] for the formation of cyclic organics may be proposed to account for the carbon insertion reactions reported in this paper. The initial step in both the monocarbon and dicarbon insertion reactions would again involve the nucleophilic attack of the anion at the positive terminal carbon of the alkynes to generate an anionic σ-vinyl intermediate with the negative charge localized on the internal vinyl carbon. The structural characterization of the *arachno*-[*endo*-4-$(NCCH{=}CH)$-6,8-$S_2B_7H_8^-$] (**10**) product, in which the dithiaborane anion is directly attached to the terminal acetylenic carbon, provides additional support for such a reaction step. Once formed, this intermediate could then react, depending upon the nature of the polyhedral anions, in two different ways, ultimately leading to either monocarbon or dicarbon insertions. Thus, as shown by path A in Scheme I, intramolecular transfer of one acidic proton to the vinylic carbon anion followed by a cyclization reaction could occur to incorporate the terminal carbon into the cluster. In this case, the internal carbon of the olefin would be converted to an exopolyhedral methylene. Alternatively, as shown in path B, the formation of a new bond between the internal carbon and an electrophilic site in the cluster could occur resulting in cyclization at the internal carbon and dicarbon insertion. In this case, the terminal carbon would be incorporated as a cage(bridging)-CH_2 fragment.

Monocarbon insertions were observed in the reactions of *arachno*-6,8-$C_2B_7H_{12}^-$ with cyanoacetylene, methyl propiolate, or 3-butyn-2-one. A reaction sequence consistent with that given in Scheme IA is illustrated in Scheme II. Previous studies[44] have shown that in the *arachno*-6,8-$C_2B_7H_{12}^-$ anion, the negative charge is localized on a cage carbon. Nucleophilic attack of the *arachno*-6,8-$C_2B_7H_{12}^-$ anion at the cyanoacetylene terminal

(34) Thompson, M. L.; Grimes, R. N. *J. Am. Chem. Soc.* **1971**, *93*, 6677–6679.

(35) (a) Plumb, C. A.; Carroll, P. J.; Sneddon, L. G. *Organometallics* **1992**, *11*, 1665–1671. (b) Plumb, C. A.; Carroll, P. J.; Sneddon, L. G. *Organometallics* **1992**, *11*, 1672–1680. (c) Plumb, C. A.; Sneddon, L. G. *Organometallics* **1992**, *11*, 1681–1685.

(36) Greatrex, R.; Greenwood, N. N.; Kirk, M. *J. Chem. Soc., Chem. Commun.* **1991**, 1510–1511.

(37) Another tricarbaborane, *nido*-5,6,10-$(CH_3)_3C_3B_7H_9$, was reported, but was later discovered to be a tetracarbaborane, see: (a) Štíbr, B.; Jelinek, T.; Janoušek, Z.; Heřmánek, S.; Drdáková, E.; Plzák, Z.; Plešek, J. *J. Chem. Soc., Chem. Commun.* **1987**, 1106–1107. (b) Štíbr, B.; Jelinek, T.; Drdáková, E.; Heřmánek, S.; Plešek, J. *Polyhedron* **1988**, *7*, 669–670. (c) Štíbr, B. *Chem. Rev.* **1992**, *92*, 225–250.

(38) The formal $R_4C_3B_2H^{3-}$ anions derived from the diborole heterocycles developed by Siebert also fall into the *arachno* electronic class, but the neutral *arachno*-$R_4C_3B_2H_4$ is not known. See, for example: (a) Siebert, W. *Angew. Chem., Int. Ed. Engl.* **1985**, *24*, 943–958. (b) Siebert, W. *Pure Appl. Chem.* **1987**, *59*, 947–954. (c) Siebert, W. *Pure Appl. Chem.* **1988**, 1345–1348. (d) Attwood, A. T.; Fonda, K. K.; Grimes, R. N.; Brodt, G.; Hu, D.; Zenneck, U.; Siebert, W. *Organometallics* **1989**, *8*, 1300–1303. (e) Brodt, G.; Kuhlmann, T.; Siebert, W. *Chem. Ber.* **1989**, *122*, 829–831.

(39) (a) Grimes, R. N. *Acc. Chem. Res.* **1983**, *16*, 22–26. (b) Grimes, R. N. *Adv. Inorg. Chem. Radiochem.* **1983**, *26*, 55–117.

(40) Hosmane, N. S.; Dehghan, M.; Davies, S. *J. Am. Chem. Soc.* **1984**, *106*, 6435–6436.

(41) Donaghy, K. J.; Carroll, P. J.; Sneddon, L. G. In preparation.

(42) (a) Wiesboeck, R. A.; Hawthorne, M. F. *J. Am. Chem. Soc.* **1964**, *86*, 1642–1643. (b) Hawthorne, M. F.; Young, D. C.; Garrett, P. M.; Owen, D. A.; Schwerin, S. G.; Tebbe, F. N.; Wegner, P. A. *J. Am. Chem. Soc.* **1968**, *90*, 962–868.

(43) (a) Bohlmann, F.; Bresinsky, E. *Chem. Ber.* **1964**, *97*, 2109–2117. (b) Dickstein, J. I.; Miller, S. I. In *The Chemistry of the Carbon-Carbon Triple Bond*; Patai, S., Ed., Wiley: New York, 1978, Chapter 19, pp 813–955.

(44) (a) Tebbe, F. N.; Garrett, P. M.; Hawthorne, M. F. *J. Am. Chem. Soc.* **1966**, *88*, 607–608. (b) Tebbe, F. N.; Garrett, P. M.; Hawthorne, M. F. *J. Am. Chem. Soc.* **1968**, *90*, 869–879.

Scheme II. Proposed Reaction Sequence Leading to Monocarbon Insertion in the Reaction of *arachno*-6,8-$C_2B_7H_{12}^-$ with Cyanoacetylene

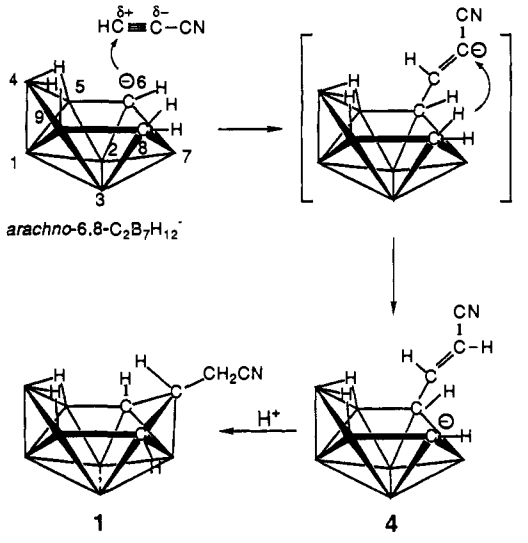

Scheme III. Proposed Reaction Sequence Leading to Dicarbon Insertion in the Reaction of *nido*-5,6-$C_2B_8H_{11}^-$ with Methyl Propiolate

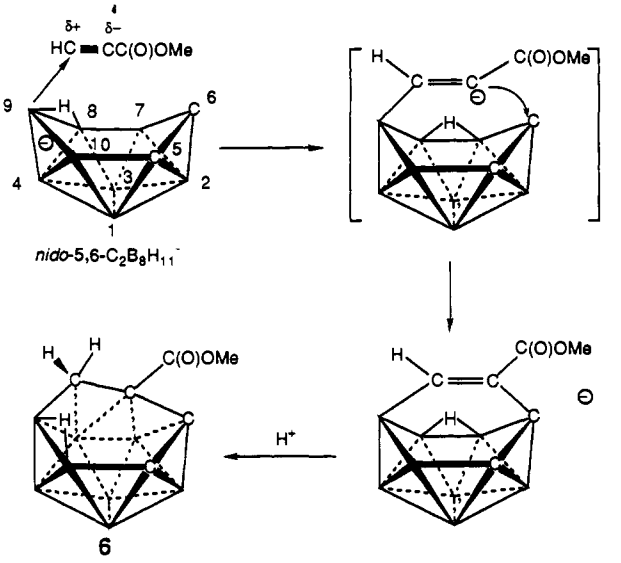

carbon, accompanied by hydrogenation of the acetylenic bond, should then produce a carbon-substituted σ-vinyl anionic product. Such an anion, **4**, was, in fact, isolated as the sole product of the reaction before the acidification step and the spectral data are consistent with the structure proposed in the figure. Subsequent acidification of **4** results in monocarbon insertion to produce the tricarbaborane **1** containing the exopolyhedral $NCCH_2$ substituent at C6. Similar types of σ-vinyl intermediates, formed in the reactions of 4,5-$C_2B_7H_{13}$ with acetylene, have been proposed to be precursors to products containing cage-inserted CH_2 groups.[37a,b] As indicated in Scheme II, the negative charge in **4** should be localized at the C8 cage carbon; however, it was found that acidification of **4** with DCl leads to deuterium incorporation at the cyano-substituted olefinic carbon. This observation suggests that either the proton (or deuteron) adds directly to the olefin or, alternatively, if it adds to C8, then the carbon-insertion process involves the subsequent addition of an *endo*-C8-H unit to the olefin. The latter step should then result, as observed in **1**, in the inserted carbon occupying a position bridging the two original cage carbons.

A reaction sequence leading to dicarbon insertion which is based on that of Scheme IB is illustrated in Scheme III for the reaction of *nido*-5,6-$C_2B_8H_{11}^-$ with methyl propiolate. Deprotonation of *nido*-5,6-$C_2B_8H_{12}$ results in the removal of one bridge proton and enhanced electron density at both the B8–B9 and B9–B10 edges. Thus, the initial reaction of *nido*-5,6-$C_2B_8H_{11}^-$ with methyl propiolate should result in the production of a B9-bonded σ-vinyl anionic intermediate which could then rearrange to an alkenyl-bridged compound. On the basis of the ^{11}B NMR spectrum of the reaction mixture, such a compound appeared to form, but it was too unstable to be isolated and characterized. In accord with Scheme IB, acidification of the reaction mixture then resulted in the formation of the dicarbon insertion product *arachno*-8-($CH_3OC(O)$)-7,8,9,10-$C_4B_8H_{13}$ (**6**), in which the terminal carbon is incorporated in the cage as a CH_2 group. In the reaction of *nido*-$B_{10}H_{13}^-$ with cyanoacetylene, carbon insertion without acidification was observed, presumably because intramolecular transfer of an acidic bridging hydrogen occurs.

Whether mono- or dicarbon insertion is observed in these reactions (i.e. path A or B) appears to depend largely on the structure and the reactivity of the polyhedral anion. The fact that the products derived from the reactions of *arachno*-6,8-$C_2B_7H_{12}^-$ are tricarbaboranes may arise as a result of both the acidity of the *endo*-C8H proton and the proximity of the C8 carbon to the σ-vinyl group, thereby making addition to the olefin possible. On the other hand, in 5,6-$C_2B_8H_{11}^-$ and $B_{10}H_{13}^-$, an additional electrophilic site (i.e. C6, B9) exists on the opposite side of these molecules, which facilitates the two-carbon insertions.

The mechanism leading to the degradative formation of **8** and **9** remains unclear. In the reaction of $B_{10}H_{13}^-$ with methyl propiolate a small amount of *arachno*-8-(MeOC(O))-7,8-$C_2B_{10}H_{14}^-$ was formed. However, the possibility that the reactions occur through the degradation of *arachno*-8-(RC(O))-7,8-$C_2B_{10}H_{14}^-$ (R = C(O)Me, C(O)OMe) can be ruled out, since the ratio of *arachno*-8-(MeOC(O))-7,8-$C_2B_{10}H_{14}^-$ to **8** did not change, even if the reaction mixture was heated at reflux in the presence of 3-butyn-2-one for longer times. Furthermore, no cage degradation product was obtained when **7** was refluxed with 3-butyn-2-one. These observations suggest that the two products were formed by independent reaction pathways.

In conclusion, the results described in this paper have demonstrated an important new synthetic pathway by which mono- or dicarbon insertions into polyhedral boron clusters may be attained. Furthermore, the use of this approach has been shown to allow the synthesis of a number of new types of carborane clusters, most notably the *arachno*-tricarbaboranes and the *arachno*-12-vertex, di- and tetracarboranes, not accessible by conventional carborane-forming reactions. This synthetic method may now result in an even wider array of new carboranes as it is applied to reactions with other polyhedral borane anions. We are presently exploring these possibilities along with the chemistry of the many unique carborane clusters that have already resulted.

Acknowledgment. We thank the National Science Foundation for the support of this research.

Supplementary Material Available: Tables of calculated hydrogen positional parameters, anisotropic temperature factors, bond distances, bond angles, and least square planes (49 pages); listing of structure factors (81 pages). Ordering information is given on any current masthead page.